3

BRIDGE WEIGH IN MOTION SYSTEMS

3.1 INTRODUCTION

A Bridge Weigh In Motion (B-WIM) system is based on the measurement of the deformation of a bridge and the use of the measurements to estimate the attributes of passing traffic loads. This technology generally consists of devices for measuring the strain caused in the bridge by the vehicles, axle detectors for collecting information on vehicle velocity and axle spacing, and data acquisition equipment. Details of a typical installation will be given in Chapter 4. The information provided by strain sensors and axle detectors is converted into axle weights through the application of an algorithm. This algorithm obtains truck weights by comparing theoretical models to a measured response. This chapter introduces existing ways to carry out this calculation while new algorithms will be developed in Chapter 7.

In the 1970's in the USA, the Federal Highway Administration (FHWA) started studying the use of Bridge WIM systems to acquire WIM data. Moses (1979) introduced an algorithm based on the assumption that a moving load will cause a bridge to bend in proportion to the product of the load magnitude and a reference curve representative of the bridge behaviour, the influence line. In the 1980's, Peters (1984) developed AXWAY in Australia. This B-WIM system is based on the same concept of influence line. A few years later, he derived a more effective system for weighing trucks using culverts, known as CULWAY (Peters 1986). Both the American and Australian systems have been used for commercial applications on bridges and culverts. Bridge Weighing Systems Inc. developed one of the first commercial B-WIM systems in 1989 on the basis of Moses' algorithm (Snyder 1992). In the 1990's, three new independent B-WIM systems were developed in Ireland, Slovenia and Japan (O'Connor 1994, Žnidaric & Baumgärtner 1998, Ojio et al. 2000).

B-WIM systems have not been widely used in Europe to date due to some limitations such as: a) durability problems due to wear and tear of axle detectors, b) restrictions on bridge type, c) Inaccuracy due to bridge and truck dynamics and d) extreme sensitivity to errors in axle spacing, influence line and/or speed. Recent progress through the European COST323 action and the WAVE project (O'Brien et al. 1999a) and other researchers have led to significant improvements in the performance of B-WIM systems in many situations that were problematic in the past. Developments include new dynamic algorithms (O'Connor & Chan 1988a, 1988b, Dempsey et al. 1998b), use of optimisation techniques (Dempsey et al. 1998a, 1999a), algorithms based on the use of multiple sensor locations (Kealy 1997), extension to other bridge types (Žnidaric et al. 1998, 1999b, Dempsey et al. 1998a, 1999a), and Free of Axle Detector (FAD) systems that allow velocity and axle spacings to be found purely from strain measurements, removing the need for axle detectors (Gagarin et al. 1994, Žnidaric et al. 1999a). This chapter reviews these developments while new approaches are in the subject of later chapters.

3.2 GENERAL CHARACTERISTICS OF BRIDGE WEIGH IN MOTION SYSTEMS

Figure 3.1 illustrates the components of a B-WIM installation: Instrumented beams giving information on the bridge response to the passing of a vehicle, axle detectors locating the vehicle in time and giving information on its dimensions, and finally hardware and software to process all this information.

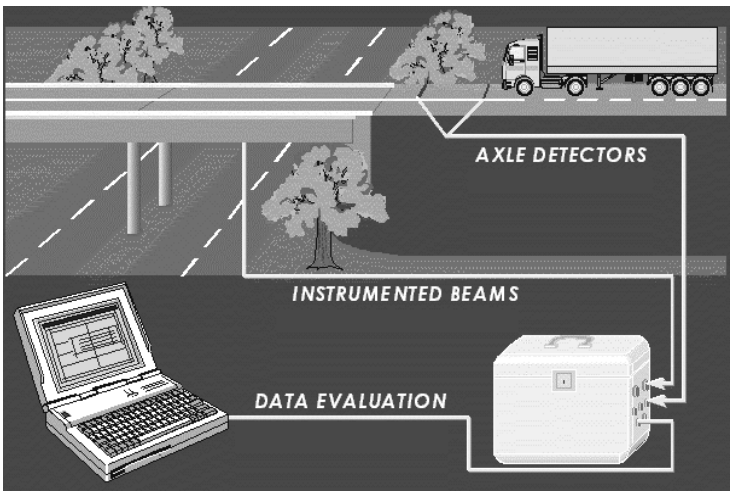

Figure 3.1 – General overview of a B-WIM system (after O'Brien et al. 1997)

3.2.1 Advantages

Both Pavement and Bridge WIM systems use the information on voltage supplied by measuring devices to work out applied load through algorithms. However, there are some noticeable differences:

- From the point of view of the installation: Most WIM systems are based on weighing detectors embedded into the pavement. A B-WIM system only requires minor traffic disruption when using portable axle detectors on the road surface. In the case of free-of-axle-detector (FAD) B-WIM systems, the interruption of traffic is not necessary at all. First applications of FAD systems on orthotropic decks and short concrete slab bridges are very promising (Jacob et al. 2000). Another feature of B-WIM is the relatively low cost of the installation: They use an existing bridge and strain transducers can be bolted to the bridge and reused. The portability of the monitoring instrumentation allows for the surveying of many sites for heavy vehicles.
- From the point of view of maintenance: As for all WIM systems, B-WIM is more accurate when the road surface is very smooth. The maintenance of the road in a good condition is much easier in B-WIM systems, as the weighing sensor is not mounted in or on the road surface. Measurement devices in B-WIM systems are not as sensitive to weather conditions (with appropriate strain sensors compensating for temperature changes), aging or deterioration due to traffic as other WIM systems. If the characteristics of the site allow for a FAD system, durability will be further improved.
- From the point of view of vehicle dynamics: B-WIM systems are not as sensitive to truck dynamic oscillations. Pavement WIM systems measure an instantaneous force for the time the tyre is supported on the WIM sensor. This time depends on the sensor width and vehicle speed and only a small portion of the tyre oscillation is recorded (a few milliseconds). The deviations above or below the static value could be in excess of 15% on a pavement in ‘good’ condition (Huhtala 1999). If a WIM system was able to measure the load for a full period of the lowest frequency, the problem of dynamic oscillation would be overcome. The only existing WIM system able of achieving this uninterrupted record is a B-WIM system. B-WIM systems measure truck forces continuously as the truck travels on the bridge. As the bridge length increases, the period of measurement increases and lower frequency components of the force can be successfully detected. This is simply not possible in pavement strip sensors due to the

very short period of measurement. Pavement WIM systems try to reduce the effect of truck dynamics through the choice of a very good road site, a frequent re-surfacing and the use of new techniques involving multiple sensors (Section 2.4.5).

B-WIM systems are often more difficult to detect by a driver than other WIM systems, as there is hardly any visible indication of instrumentation (primarily located under the bridge). These unbiased B-WIM measurements supply information that can be used for purposes other than WIM. For instance, raw data used for bridge monitoring (as carried out in the Tagus suspension bridge in Lisbon) or storage for further processing (such as fatigue calculation).

In addition to the factors given in the preceding paragraph, if truck mass is negligible compared to bridge mass, truck dynamic effects on measurements are reduced by the bridge inertia. A truck can be easily located on a lot of existing bridges in the same way a typical static weighing scale would do. The difference is the existence of the bridge and truck dynamic behaviour. If bridge dynamics are removed efficiently, the result in gross vehicle weight should be clearly very accurate. In the case of culverts and bridges with very short spans, bridge dynamics are negligible.

3.2.2 Disadvantages

In order for B-WIM to be implemented, there is a need for the presence of a suitable bridge in the route of interest. A previous test using trucks with loading close to the expected mean gross weight should be run to analyse the suitability of a bridge for a given WIM purpose. Results with unloaded, full and half-loaded vehicles at different speeds should not exhibit any inconsistency or non-linearity depending on their speed or weight (Jacob et al. 2000). If there is non-linearity, input parameters must be checked or correction functions applied. A 2-axle or 3-axle rigid truck is useful to identify the existence of dynamic problems (i.e. a poor pavement or a bump). Results should indicate what accuracy class could be expected for that site. Some bridges might not even qualify for a B-WIM installation. For instance:

- If the bridge is too stiff, the existing instrumentation might not be able to measure any significant strain induced by the load.

- If the bridge is too long, accuracy will decrease, as there could be a lot of vehicles crossing the bridge simultaneously. Therefore, the bridge is less likely to qualify for FAD, as it will be very difficult to distinguish the effect of individual axles. Further, no known B-WIM system has yet been developed to cater for multiple vehicle presence. Spans shorter than 20 m are generally preferred for most B-WIM systems and bi-directional traffic, though spans up to 40 m can be used if axles from a group are not an important issue (Žnidaric & Baumgärtner 1998).
- If the weight of the moving load is low, there can also be difficulties recording a significant strain.
- If the bridge is too skew, there is a possible influence of lateral positioning of the vehicle, that must be taken into account. Žnidaric and Baumgärtner (1998) suggest even angles up to 45º can be acceptable, except in the case of bridges with measured span shorter than its width (i.e., culverts, where skewness is not recommended at all).
- If the bridge has a lot of lanes, the effect of a single axle will be very difficult to distinguish from axles present in other lanes simultaneously.
- If the bridge section is too thick, strain peaks are smoothed out, and the site might not qualify for FAD.
- Many B-WIM algorithms assume a constant speed along the bridge, so sites where this does not occur should be avoided (i.e. where traffic jams are likely or in very long bridges).

The system is usually more accurate for GVW than axle weights. Further, it is difficult to distinguish individual axle weights inside closely spaced axle combinations (tandems or tridems). While results for Gross Vehicle Weight are expected to be very accurate, the determination of axle weights is more difficult. The effect of all the vehicle axles on a bridge is measured simultaneously and it is necessary to differentiate the contribution of each axle based on knowledge on the bridge-truck structural system. If there is a single vehicle travelling on a bridge, only the effect of the first and last axle can be measured individually for a very short period of time, i.e., when entering and leaving the bridge respectively. This difference in accuracy for GVW and axle weights does not apply to culverts or very short span bridges, where it is possible to weigh axles or axle groups individually.

Depending on the algorithm adopted, a BWIM system requires a prior knowledge of the bridge structural behaviour, i.e., the influence line for the bending moment at the sensor location. A larger difference between assumed and real bridge behaviour will result in higher errors in results. Better results can be obtained when the bridge model is adapted using measured strains at the site during calibration. The necessity for this model makes B-WIM systems require more computation time per vehicle than a pavement WIM system, though modern computers can generally allow for calculation in real time.

It has also been found that accuracy decreases in the cases where the first natural period of the bridge is greater than the time taken for the truck to cross the bridge. Low-pass filtering could reduce the influence of dynamics, but this technique is not recommended except for very high frequencies, as important static components can be removed in the case of very closely spaced axles and/or high vehicle speeds.

Existing known B-WIM Systems can only weigh a single vehicle on the bridge. Interference from other vehicles decreases accuracy. For this reason, the AXWAY system limits its use to traffic densities below 500 trucks per hour. The problem with high traffic densities is the possibility of simultaneous traffic events: vehicle whose weight is being measured might be overweighed due to the presence of vehicles in adjacent lanes.

3.3 MOSES' ALGORITHM

First approaches in the USA in the early 1970's used highway bridges as weighing scales. They measured and related the maximum peak strain recorded during the truck crossing to its GVW. Acceptable results were obtained, but this correlation was only valid when applied to the same vehicle type. It was quickly noticed that axle detectors mounted on the road surface were necessary for:

- Distinguishing the vehicle type by number of axles and spacings
- Introducing new algorithms that require number of axles, spacings and speed in their formulation. The objective of these algorithms is to achieve: (a) an improved accuracy in GVW, taking into account the small differences of weight distribution between axles that affected the magnitude of the maximum strain peak; (b) results for individual axle weights.

As result, Moses (1979) developed a system that used instrumented bridge girders combined with timings from axle detectors to predict the axle and gross weights of trucks in motion. This prediction is based on the fact that a moving load along a structure will set up stresses in proportion to the product of the value of the influence line and the axle load magnitude. An influence line is defined as the bending moment at the point of measurement due to a unit axle load moving along the bridge. At this time, Moses proved that weight predictions were feasible and results were repeatable when using a calibration truck. The bridge WIM system described by Moses was the first of its kind and nowadays it is widespread in the USA and elsewhere. FASTWEIGH is an American B-WIM system that uses Moses' algorithm, giving on site readings through a matrix solution technique.

3.3.1 Ideal Site

First bridges used for weighing purposes were composed of multiple beams and a slab. The reason for the choice of this type of bridge was its length and relative stiffness in the longitudinal direction compared to the transverse one. These longitudinal beams primarily carry the traffic loads. Therefore, all girders are usually identical, though some differences in section modulus can appear in edge members. The simplest bridge to apply Moses' algorithm would be a single span beam-and-slab bridge with no skew. Studies prior to Moses (1979) indicated a sequence of single spans less than 18 m as an ideal bridge length to predict axle weights. A larger span, over 24 m, would be preferable for determining GVW. Moses tested his algorithm in a 3-span continuous bridge, and his optimisation process showed no statistically significant advantage to either span for weight prediction. In fact, best results were achieved by averaging predictions obtained from each set of gauges at different longitudinal locations. Other bridges could be used for WIM, once an influence line of the bending moment can be obtained and the relation between measurements and this influence line is reliable. Thus, concrete slab bridges, trusses, skew girders or orthotropic decks can also be instrumented for weighing purposes.

3.3.2 Principle

If a vehicle is considered at a certain static position on the bridge, there will be a relation between the strain (ε_i) generated at strain transducer i, and the bending moment (M_i) given by:

$$M_i = ES_i\varepsilon_i \tag{3.1}$$

where E is modulus of elasticity and S_i section modulus of the ith girder.

The total bending moment (M) will be given by the sum of all strain transducers at each girder i transversely for a given longitudinal location as:

$$M = \sum_{i=1}^{no\_girders} M_i = \sum_{i=1}^{no\_girders} ES_i\varepsilon_i \tag{3.2}$$

As Moses' algorithm is based on a one-dimensional approach, the signal from all sensors in different transverse locations and the same longitudinal location are added. The difference in section modulus induces an error in this sum. However, this effect is not significant due to the smaller load carried by the outer members and the fact that the truck will always run in the same transverse location within the lane. So, if E and S_i are assumed to be constant for each girder, then

$$M = ES\sum_{i=1}^{no\_girders}\varepsilon_i \tag{3.3}$$

Thus, total bending moment and measured strain are directly related by the product of two constants (ES), which is independent of vehicle position. In theory, this constant can be calculated from bridge dimensions and material properties, but in practise, it is derived from measuring the effect of the crossing of a truck of known weight over the bridge.

This total bending moment (M) can be related to the individual axle weights for each vehicle position. Then, the total number of unknowns (N), number of axles, can be calculated from a knowledge of N strain records corresponding to N different positions of

the truck along the bridge. This system of equations requires the use of the influence line of the bending moment for that bridge location. The ordinate of the influence line indicates the bending moment for a unit axle load located at a certain point along the bridge. An advantage of using beam-and-slab bridges is that generally their real behaviour corresponds well with simple influence lines based on simple beam theory. The influence line can also be found by crossing a calibration vehicle of known weights slowly across the bridge while recording the strain. Figure 3.2 illustrates the unknowns and the input data that is necessary for the calculation of axle weights in a B-WIM algorithm.

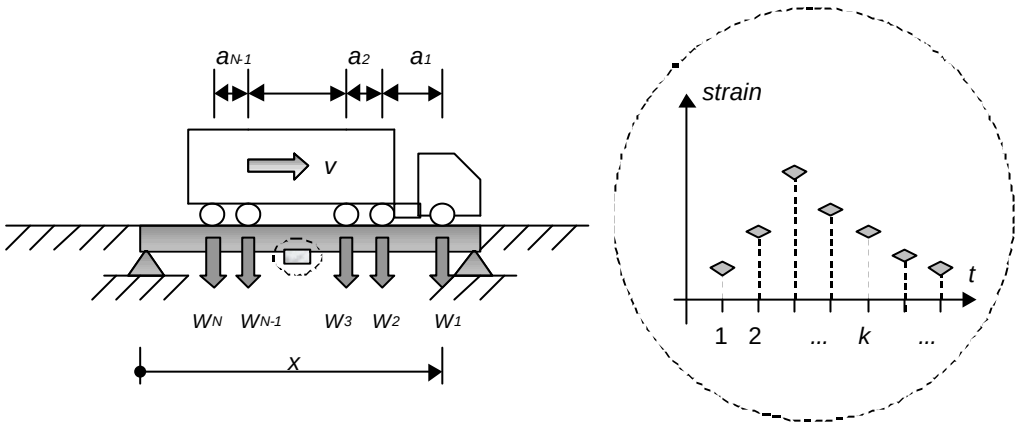

Figure 3.2 – Parameters involved in a B-WIM algorithm

If the first axle is located at a distance x from the support, the bending moment is:

$$M(x) = W_1 I(x) + W_2 I(x - a_1) + W_3 I(x - a_1 - a_2) + \ldots \tag{3.4}$$

i.e.,

$$M(x) = \sum_{i=1}^{N} W_i I(x - \sum_{j=1}^{i-1} a_j) \tag{3.5}$$

where $I(\ )$ is the influence ordinate.

As real strain is being sampled at discrete time intervals, for a further comparison in the same terms, the theoretical moment (M) can be expressed as a function of time t_k, where k

is the reading number. The total number of readings is related to the frequency at which measurements take place.

$$M(t_k) = \sum_{i=1}^{N} W_i I\left(t_k - \frac{\sum_{j=1}^{i-1} a_j}{v}\right) \tag{3.6}$$

where v is velocity. The value of the influence line as a function of time ($I_i(t_k)$) can be calculated for each axle i from axle spacings and speed. This speed is obtained from the axle detectors and assumed to be constant along the bridge.

3.3.3 Removal of Dynamics

Up to this point, the theoretical static response of the bridge ($M(t)$) has been presented. In reality, bridge response is not static, but oscillates around a static position of equilibrium as shown in Figure 3.3.

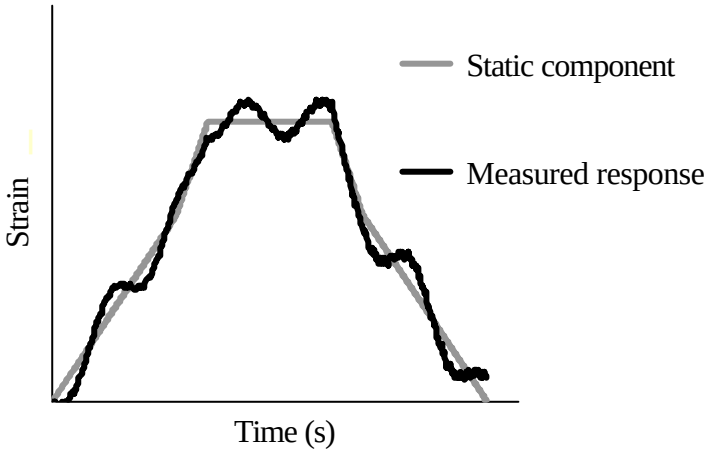

Figure 3.3 – Theoretical static strain ($M(t_k)$) versus typical measured strain ($\tilde{M}(t_k)$) at midspan

Moses uses the fact that a lot of measurements are available during the truck crossing to smooth out the dynamic component. This is achieved by minimising an error function $\boldsymbol{j}$, defined as follows:

$$j = \sum_{k=1}^{T} [M(t_k) - \tilde{M}(t_k)]^2 \tag{3.7}$$

i.e.:

$$j = \sum_{k=1}^{T} [\sum_{i=1}^{N} W_i I(t_k - \frac{\sum_{j=1}^{i-1} a_j}{v}) - \tilde{M}(t_k)]^2 \tag{3.8}$$

where $\tilde{M}(t_k)$ is the measured strain and T is the number of scans while the truck is on the bridge. A minimum condition is imposed by:

$$\frac{\partial j}{\partial W_i} = 0 \qquad ; \qquad i = 1,2,\ldots N \tag{3.9}$$

This gives:

$$\sum_{k=1}^{T} [2(\sum_{j=1}^{N} W_j I(t_k - \frac{\sum_{r=1}^{j-1} a_r}{v}) - \tilde{M}(t_k)) I(t_k - \frac{\sum_{r=1}^{i-1} a_r}{v})] = 0 \quad ; \quad i = 1,2,\ldots,N \tag{3.10}$$

And re-ordering:

$$\sum_{k=1}^{T} \left[\sum_{j=1}^{N} W_j I(t_k - \frac{\sum_{r=1}^{j-1} a_r}{v}) \right] I(t_k - \frac{\sum_{r=1}^{i-1} a_r}{v}) = \sum_{k=1}^{T} \tilde{M}(t_k) I(t_k - \frac{\sum_{r=1}^{i-1} a_r}{v}) \quad ; \quad i = 1,\ldots,N \tag{3.11}$$

which is equivalent to using a least-squares fitting method of measurement to theory to find axle weights. Equation 3.8 can be expressed in matrix form as:

$$[F]_{NxN} \{W\}_{Nx1} = \{B\}_{Nx1} \tag{3.12}$$

where:

$$[F_{ji}] = \sum_{k=1}^{T} I(t_k - \frac{\sum_{r=1}^{j-1} a_r}{v}) I(t_k - \frac{\sum_{r=1}^{i-1} a_r}{v}) \tag{3.13}$$

$$\{B_i\} = \sum_{k=1}^{T} \tilde{M}(t_k) I(t_k - \frac{\sum_{r=1}^{i-1} a_r}{v}) \tag{3.14}$$

and *{W}* is the vector of unknown axle weights.

[F] only depends on the influence line, axle spacing and speed, while *{B}* depends on the same factors and measured strain as well. Finally, axle weights *{W}* can be found by:

$$\{W\} = [F]^{-1}\{B\} \tag{3.15}$$

Gross vehicle weight is found by summing individual axle weights:

$$GVW = \sum_{i=1}^{N} W_i \tag{3.16}$$

Therefore, Moses recommends combining axle weights when there is a tandem group. He also emphasised that the accuracy of calculated weights is highly sensitive to an accurate estimation of axle spacings and in particular, speed.

3.4 ALLIED STATIC ALGORITHMS FOR CALCULATION OF WEIGHTS

AXWAY is a system developed by Peters (1984) in Australia in the early 1980's. As with Moses' algorithm, AXWAY relies on an influence line as a good reference of the strain caused in a bridge by the vehicle weight. When culverts were tested, results indicated that a simpler and better system could be developed for these structures (Peters 1986). This system, called CULWAY, uses existing concrete culverts and obtains truck masses from measured strain through a unit influence line algorithm. Nowadays, CULWAY dominates the Australian highway speed WIM market with around 150 installations and systems in

China, Malaysia and New Zealand. This section also introduces a novel method developed by Dempsey (1997) for calculating gross vehicle weights.

3.4.1 AXWAY

Peters (1984) assumes that total strain is proportional to the applied load due to the linear elastic nature of bridge material. This system was tested in a single span slab bridge first. Strain measurements from conventional strain gauges were not high and consistent enough for weighing purposes. The need arose for the development of mechanical strain amplifiers that amplified the actual strain about ten times. Considerable progress was also made in the durability and reliability of axle detection systems. Though AXWAY uses the same concept of unit influence line as Moses, there are some differences in the final calculation of weights that will be reviewed in this section.

Ideal site

Peters suggests:

- Single span quite short to ensure a high probability of having only one vehicle on the bridge at a time.
- A linear strain response. The measured strain should also be sufficiently large (0.5 με/ton of vehicle weight).
- One or two lanes preferably.
- Bridge dynamic characteristics should allow for at least four vibration periods per vehicle pass.
- A relatively smooth roadway surface is required both prior to and on the bridge to reduce vibration amplitudes.

Determination of the influence line

Strains are measured at midspan and all strains across the bridge at this point are added together. The sum of all such strains should give the same total regardless of the transverse position of the truck in a lane. Most bridges are quite wide and tend to act as plates rather than beams, and so, the influence line for locations in different lanes will be quite different. Accordingly, this influence line is calculated by applying the theory of bending plate for

that particular bridge. The magnitude of this unit influence line can be obtained by measuring the strain caused by a truck of known axle weights.

Technique to remove dynamics

Every bridge has a main mode of vibration corresponding to its first natural frequency. The amplitude of this vibration depends on the dynamic characteristics of the bridge. The removal of this component prior to the weight calculation should improve the accuracy of the final results.

Peters proposed a moving average technique based on the assumption that the total strain response is a combination of the vehicle response and the bridge vibration at its natural frequency. If the vibrations on certain bridges do not oscillate around a static position, then this filtering technique might not be suitable. If this vibration is a sinusoidal wave of constant natural period, even if there is a gradual change in wave amplitude, the integral of the bridge vibration over any integral number of periods should be zero. Peters recommends about a minimum of four periods of the bridge natural frequency for a good smoothing of the original strain signal by this technique.

As bridge vibration takes place in combination with bridge static response, the filtered signal will be the result of integrating the measured strain over the natural period at each step. As plate theory is assumed, bending at midspan is likely to take place in two directions. Hence, sharp peaks, typical in longitudinal bending of a narrow beam, do not tend to occur and the corruption of the static response by this filtering is not as significant. For instance, the spectral representation of a response with sharp peaks contains higher and more spread frequency components than a smooth response. However, part of the static component can still be removed dangerously when having very closely spaced axles and/or high speeds.

Iterative technique in the calculation of weights

Iterative techniques increase computer time, so processing of weights in real time can be difficult to achieve. Once a strain record has been obtained as a function of time and dynamics have been filtered out, the procedure to obtain the vehicle weights suggested by Peters was the following one:

- Strain is expressed as a function of the vehicle position coordinates through vehicle speed.
- GVW is assumed to be proportional to the area under the strain-position curve. The exact value for GVW is obtained from the product of this area and a weight correction factor.
- Then, axle weights are calculated. Some initial axle values are obtained by distributing GVW equally between all axles. Then, the following iterative process takes place:

[1] Generate expected response curve from axle values using unit influence line.
[2] Compare theoretical and real strain record and find greatest difference between both curves.
[3] Locate axle most likely to be causing this difference, i.e. nearest axle. Then, increase or decrease that axle weight in proportion to the magnitude of the misfit.
[4] Readjust axle weights to maintain the correct GVW.
[5] Check actual axle group weights with previous estimates.
[6] If change for all axle weights < 0.05 tonnes, solution is assumed to have been reached. Otherwise, re-start process at [1].

The correct longitudinal location of the truck on the bridge at each instant is very important for accurate weighing. An axle detector prior to the bridge acts as a trigger to start the strain record. This starting point is the same for every vehicle. A deviation between the estimated truck location and its corresponding strain record could have a very significant influence on the individual axle weights. The effect on GVW would be smaller as some axles would be overloaded and others underloaded, resulting into a compensated total weight. The correct adjustment between the axle detector, the strain record and the vehicle is carried out during calibration. A test vehicle is passed several times on each lane. Then, the likely mismatch is adjusted in intervals of 0.1 m, which is the division interval used in the algorithm. This adjustment is particularly relevant in skew bridges.

Like Moses, Peters treats loads within an axle group as if the total weight of the tandem or tridem was equally distributed between all axles in the group. Thus, though all axle weights are calculated individually, when these axles belong to an axle group, the weight obtained for each axle in a group is added together and divided between the number of axles to get the final axle weight. This is due to the difficulty of distinguishing between

closely spaced loads. Axles are considered to be in the same axle group when the spacing is less than 1.5 m for tandems or tridems, or less than 2 m for twin steers.

3.4.2 CULWAY

CULWAY (Peters 1986) uses two axle sensors to collect information on the speed and axle spacings of the vehicle (Figures 3.4(a) and (b)). These sensors also work like triggers. When the first axle of the vehicle hits the first axle sensor, the system measures the initial strain at the culvert midspan. Then, each time the second axle sensor is hit by an axle, the system measures the strain change, which is related to the axle weight.

(a) Site[9]

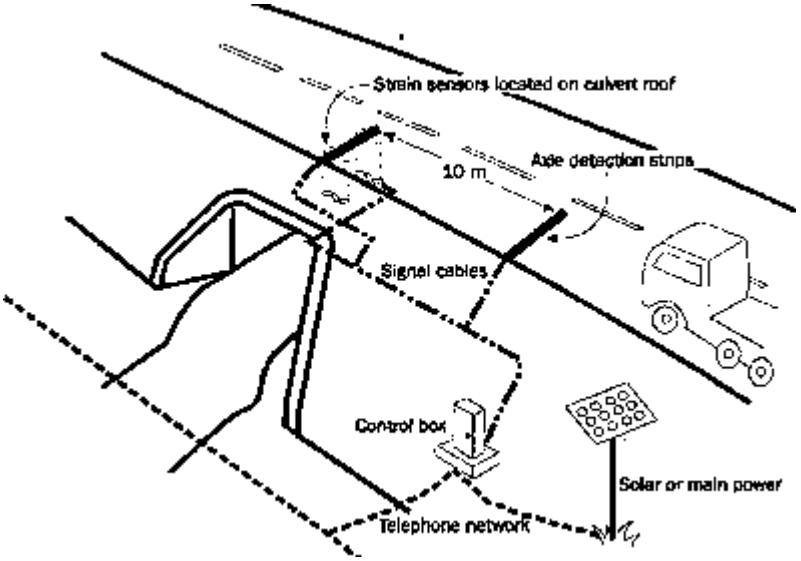

(b) Installation (after Peters 1998)

Figure 3.4 – CULWAY system

Ideal site

Peters (1986) suggests the ideal culvert would include the following features:

- Single span box culverts or reinforced concrete pipes, less than 2.7 m span. This limitation avoids more than one axle group on the culvert at a time. When there are more than one axle present at a time, the measured strain will be the sum of the contributions of the different axles.
- Good road surface. Culvert and road preferably built at the same time to avoid settlement.
- No or virtually no skew.

- Soil cover over 600 mm, but less than 1500 mm. These limits are due to the need to avoid dynamics while receiving a strain signal that is strong enough.
- Clear access to underside is required. The sensors are placed right underneath the wheel tracks on the road. If the culvert was made from precast segments with lengths of less than 1.2 m, one strain gauge per box or pipe, placed centrally, is recommended. This placement is chosen to reduce the influence of the likely different transverse position of the vehicle being weighed.
- Box culverts with continuous lid bridging two cells should be avoided to facilitate calculations.

Calculation of weights

Calibration takes place with trucks of known weights travelling at the expected speeds. Tests have indicated that the influence of speed on results is negligible. CULWAY minimises the errors due to variations in the lateral position of the vehicle by simply adding the strain response of each individual sensor.

There is a systematic error which results in underweighing of steer axles. There are several theories to explain this phenomenon: Smaller contact area of tyre, strain non-linearity of concrete or dynamic weight of steer axles inferior to the static weight due to aerodynamic and torque effect. CULWAY manages the issue with a site-specific correction function to allow for this effect. A plot is made of known single axle weights against their respective strain responses. If a non-linear effect is observed, a function is derived to correct for the misfit between the measured and static weight W_i of axle i. The function can be defined as in Equation 3.17:

$$W_i = C\varepsilon_i^{\gamma} \tag{3.17}$$

where C is a calibration factor and γ a non-linearity correction factor. C represents ratio between strain values ε_i and weights W_i, and γ will normally be 1 unless the plot suggests otherwise. It is necessary to adjust a third factor which is the length of the unit influence line. This is not necessary for measuring single axles but it is very important when there are overlapping influence of axles in groups such as tandems and tridems. The effective

influence line length should be taken as the clear span of the culvert plus twice the depth of fill unless evidence suggests otherwise.

Advantages

Some of the advantages of CULWAY systems are:

- Vibration of the culvert is virtually non-existent. Strain response is clear of the dynamic problems found in bridges. The measured strain in a culvert is mainly static, this is, purely induced by the axle mass, and to a minor extent the dynamic load of the vehicle. This is due to the total restraint by the surrounding embankment and pavement on culverts. This soil cover damps high frequency vibrations out, while being adequately stiff to transmit the wheel loads to the concrete culvert. Hence, the strain signal does not require filtering to remove any dynamics.
- WIM systems (or B-WIM) generally often have a bump or discontinuity in pavement profile as a result of the joint between the road and the road sensor (or bridge). This bump excites the truck dynamically and generates high amplitudes in the axle weight variation. There is no joint or discontinuity between the road and culvert, though some settlement might have taken place. There is no excitation of the vehicle dynamics as a result of the weighing system installation and so, the only dynamic effects are those inherent to the vehicle and the road surface profile.
- Strain sensors are located well away from the road surface. This circumstance preserves them from traffic or weather aggressiveness, and little or no site maintenance is required.

Long Term Performance

The effects of seasonal moisture, temperature and stiffness variation of the pavement materials over the culvert have been investigated by Peters (1998). Some seasonal variations in measured vehicle mass have been noticeable at some culvert sites. The concrete bends more in winter than in summer, which could be due to a change in the properties of the pavement, less stiff in winter than in summer, probably originating from a higher moisture content, temperature conditions or a combination of both. The analysis has shown the variation to be consistent from year to year. Culverts with larger cover exhibit less variation. An algorithm was designed to correct seasonal variations due to climatic factors. This algorithm applies a monthly percentage correction to all measured values.

Peters has also shown that calibration of a WIM site can be carried out with long term data at a far lower cost than regular site re-calibration. This adjustment has to be checked carefully as the seasonal differences in vehicle weights could be due to a change in loading patterns instead of climatic factors.

3.4.3 Left Slope Alignment

An alternative method to calculate gross vehicle weights of trucks was developed by Dempsey (1997). This weight is obtained by comparing the measured bridge strain due to a truck of unknown weight to that of a calibration truck by a best fit procedure. The approach minimises the squared difference between measured ($\tilde{e}$) and calibration truck (e) strain values as given in Equation 3.18,

$$\text{Minimise} \quad j = \sum_{i=1}^{n} \left[e_i - g\tilde{e}_i \right]^2 \tag{3.18}$$

where n is the number of discrete points along the bridge at which strain is being recorded and g is a scaling factor. If the solution is totally accurate, then g is the ratio of the weight of the calibration truck to that of the truck whose weight is sought.

Theoretical static bridge responses were generated for five different truck configurations. All errors were below 6% regardless of the truck chosen for calibration. It also became evident that accuracy could be improved by aligning the left hand slope of the strain responses of both trucks before minimising Equation 3.18. This aligning policy reduces the influence of gross weight distribution within the truck. It was also found that transverse offsets of trucks from that of the lane centre line of up to 1 m do not affect accuracy in a significant manner. Experimental tests proved that a dynamic calibration performs better than a static calibration. A static calibration involved a truck of known weight being positioned at different points along the span of the bridge, while the dynamic calibration was obtained from passing a truck of known weight across the bridge at various speeds.

3.5 FURTHER DEVELOPMENTS

The application of new techniques to improve the performance of a static algorithm is discussed in the following sections. These recent contributions include artificial neural networks, optimisation techniques, multiple sensors or a combined B-WIM and Pavement WIM system.

3.5.1 Sources of Inaccuracy

After analysing the results of many tests, it became evident that the parameters with the highest influence on final accuracy were (Ž nidaric and Baumgärtner 1998):

- Selection of influence line
- Accurate assessment of vehicle velocity
- Dynamics of vehicles and bridge, depending on the structure
- Calibration methods

The first three aspects are reviewed next, while the influence of calibration is discussed in Section 3.7.2.

Influence Line

Most B-WIM algorithms are based on the concept of an influence line. Figure 3.5 shows influence lines for a simply supported single-span beam (determinate structure), a fixed-ended single-span and a two-span continuous beam (indeterminate structures). The length of the influence line can extend beyond the centre-lines of the supports as shown by the discontinuous lines in Figure 3.5. The real influence line of a bridge will correspond to partially constrained rotation at the supports (between the theoretical simply supported and fixed situations represented in the figure).

The prediction of axle weights can be very inaccurate if a wrong influence line is chosen, especially in bridges with longer span. An idea of the magnitude of these errors for two different spans is given in Figure 3.6. The values of this figure are obtained by simulating a signal from an influence line between the simply supported and fixed cases, and then calculating weights when using other influence lines. While the error is below 10% for the 2 m span bridge and it is similar for GVW and axle weights, errors of several hundred percent were observed for 32-m long bridges. The greater the difference between the

integrals of measured and theoretical strains, the higher the errors in the results (Žnidaric and Baumgärtner 1998).

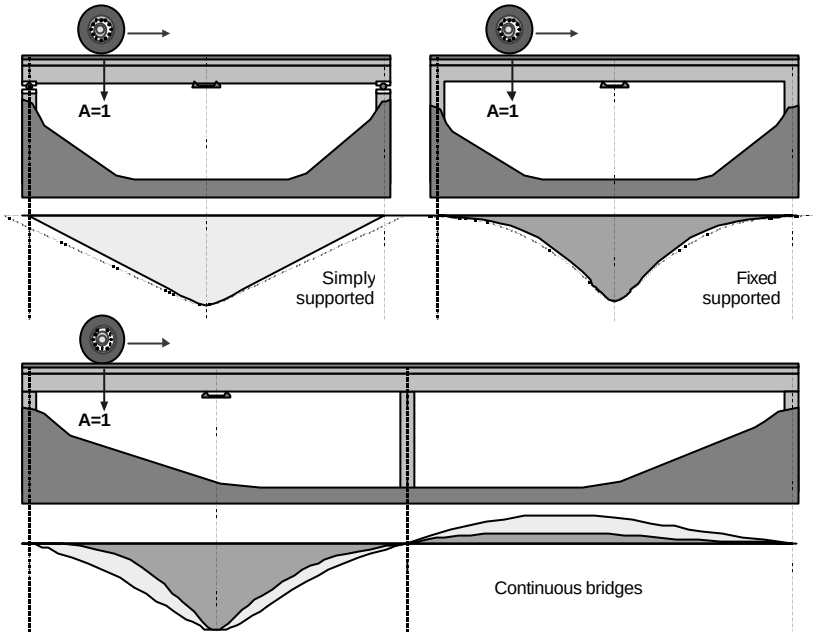

Figure 3.5 – Influence lines of bending moment at midspan for simply and fixed supported (integral) single-span bridge and for a 2-span bridge (after Jacob et al. 2000)

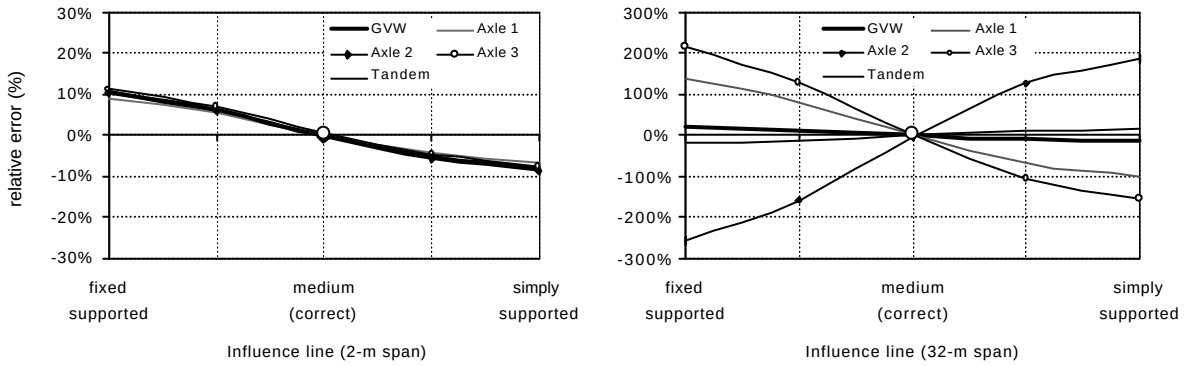

(a) 2 m span (b) 32 m span

Figure 3.6 – Errors in weights due to wrong selection of the influence line (after Žnidaric & Baumgärtner 1998)

The influence line should be corrected based on measured strains at site. Žnidaric et al (1998) and McNulty (1999) propose different methods to carry out this experimental adjustment in the Slovenian (SiWIM) and Irish (DuWIM) systems respectively. The degree of accuracy of both systems is similar as will be shown in Section 3.7.4.

Speed

Vehicle velocity is one of the most important parameters affecting the accuracy of final results. A small error in velocity can result in significant errors in weights, even in short span bridges. Several solutions have been adopted to overcome this problem (Ž nidaric & Baumgärtner 1998):

- Placement of the second axle detector above the strain transducers, i.e., further apart from the first than usual.
- Measurement of velocity at more than one location on the bridge.
- Allowance for acceleration and deceleration.
- Optimisation of the results by finding velocity, axle spacings and axle loads which minimise the difference between the theoretical and measured responses of the bridge. The results of applying this technique for a 2 m and 32 m span are shown in Figure 3.7.

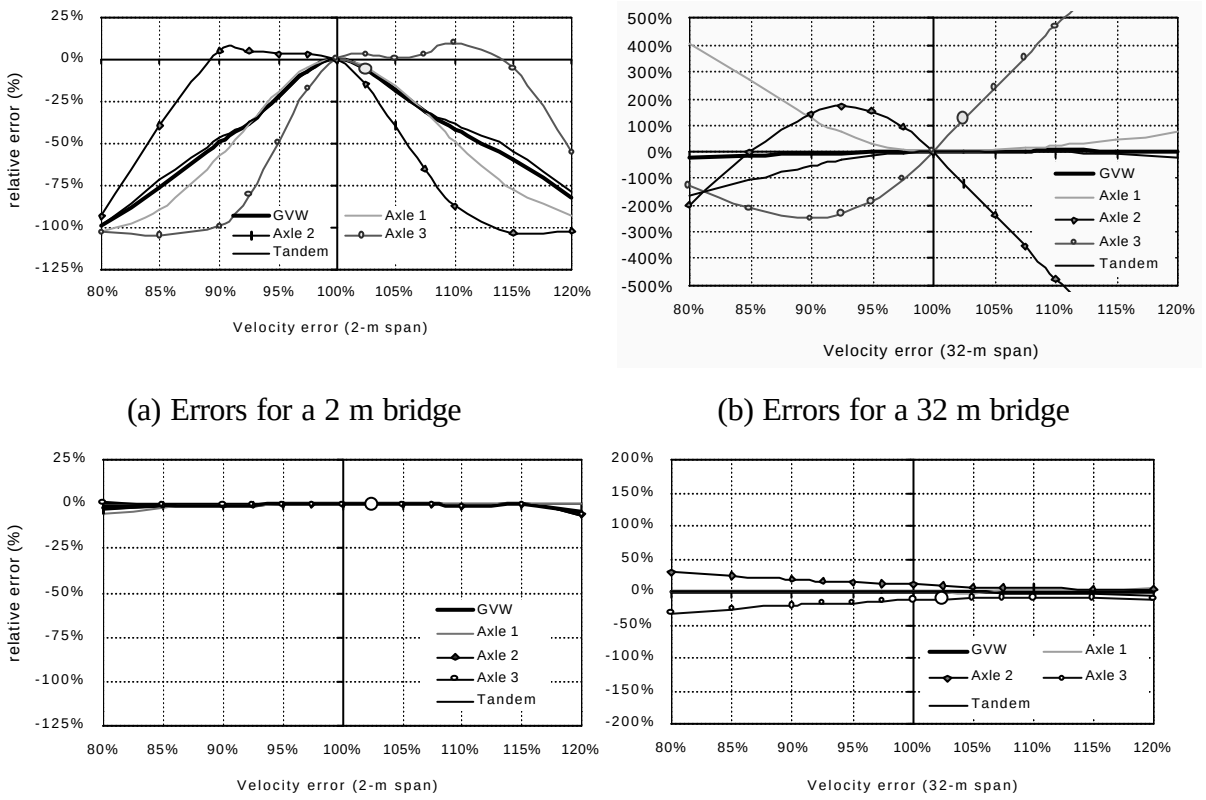

(a) Errors for a 2 m bridge

(b) Errors for a 32 m bridge

(c) Errors for a 2 m bridge after applying optimisation

(d) Errors for a 32 m bridge after applying optimisation

Figure 3.7 – Errors of weights due to an error in velocity for 2 m and 32 m long bridge (after Ž nidaric & Baumgärtner 1998)

Dynamics

Jacob et al (2000) recommend choosing bridges:

- With a smooth approach and no bump just before or on the bridge. Dynamic wheel forces up to 100% have been measured in an instrumented truck due to a bump just before the bridge (Lutzenberger & Baumgärtner 1999).
- With high eigen-frequencies. This high frequency of the bridge avoids dynamic interaction with the truck frequencies of body bouncing and pitching. If the eigen-frequency is low, a significant static component of the applied load can be removed by low-pass filtering. Figure 3.8 shows unfiltered and filtered longitudinal strain recorded in a bridge with low first natural longitudinal frequencies: 1.35 and 2 Hz.

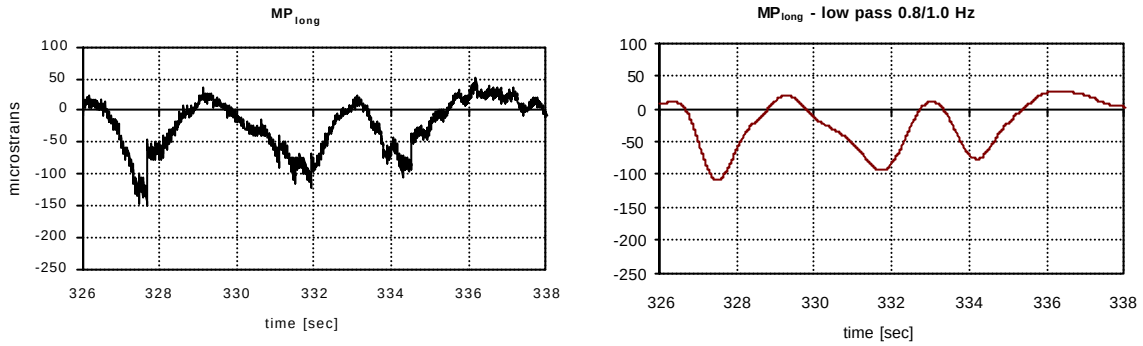

(a) Unfiltered data (b) Filtered data

Figure 3.8 – Low-pass filtering of signal (after Ž nidaric & Baumgärtner 1998)

Theoretical dynamic simulations can be used to detect likely problems or to determine the location of the sensors which minimises errors.

3.5.2 Artificial Neural Networks

Artificial Neural Networks (ANNs) are computational models based on the neural structure of the brain. The brain basically learns from experience. Gagarin et al (1994) introduce a B-WIM algorithm that uses neural networks to determine axle weights, vehicle classification and velocity purely from the strain readings taken from the bridge as the truck travels along. This procedure removes the need for axle detectors on the road surface to obtain axle spacings and velocity. This is a very relevant advantage as axle detectors mounted on the road surface are rapidly worn by heavy traffic, apart from warning drivers about the presence of instrumentation on the bridge.

The ANN architecture recommended by Gagarin is the Radial-Gaussian Incremental-Learning Network (RGIN). This architecture is based on a layered feed-forward that provides a mapping function from a vector of input values x_i (i.e., vector of measured strains at different times during the passage of the truck) to a corresponding vector of output values y_i (i.e., vector of quantities representing velocity, axle loads and axle spacings) in neighboring layers. ANN is applied to B-WIM in two network levels. A single network should be possible, but pilot experiments showed it impracticable due to the unacceptable length of the training period. Accordingly the first level, made of one network module, classifies the trucks and the second level, made of different network modules (one for each type of truck), estimates velocity, axle spacings and weights. Figures 3.9 and 3.10 represent these two layered modular structures.

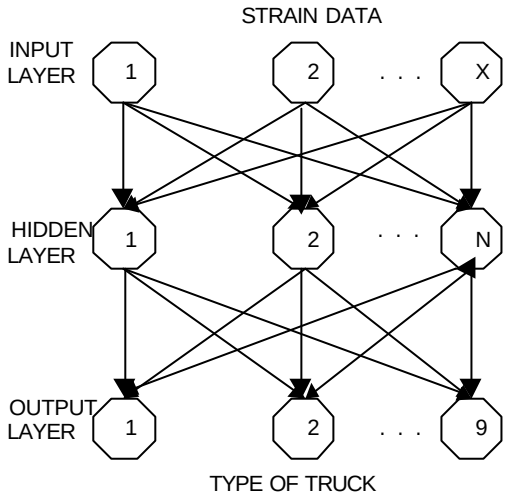

Figure 3.9 – First Level Network

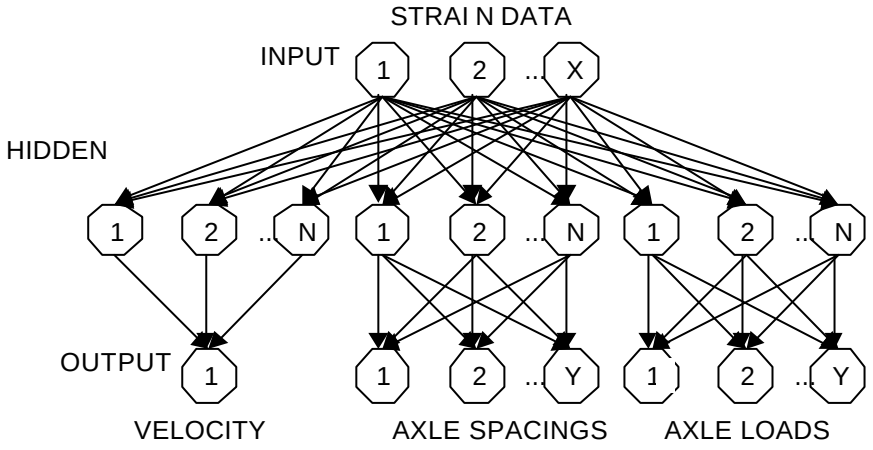

Figure 3.10 – Second Level Network

The network is trained to provide real-time assessments of truck attributes based on a variety of truck configurations and corresponding strain data. During this training, the network must develop a surface that approximates each value y_i in the output vector against its values in the input vector $\{x\}$. The output value y_q of a hidden neuron q is given by the Gaussian-shaped function:

$$y_q = \sum_{j=1}^{M} e^{\left[-s_j \sum_{k=1}^{N} (x_k - c_{km})^2\right]} w_{jq} \tag{3.19}$$

where s_j is a parameter that determines the width of the Gaussian-shaped function, c_{km} constants (known as offsets) from values passed along a link, w_{jq} weights associated with the output values, N the number of input vectors into the neuron, and M the number of output vectors.

This system is built by training one neuron at a time (represented by octagons in Figures 3.9 and 3.10). Initially, a network is set up with the required number of input and output neurons but without hidden neurons, that will be added and trained in a posterior stage until reaching a predefined level of accuracy. New neurons are added in such a way that the centroid of the generated Gaussian-shaped function will focus in regions with the highest errors. This is achieved with the correct c_{km} values. Then, w_{jq} is adjusted so that the amplitude of the Gaussian-shaped bump matches that of the error. Finally, the parameter s_j is adjusted to minimise the remaining errors. In other words, network training is essentially a surface-fitting exercise.

The truck attributes are calculated as follows: The strain is given to the first network level and values y_q are generated at each output neuron (Figure 3.9). The output with the greatest value denotes the type of truck under the assessment of the first level network. Once the type of truck is known, the appropriate module (there is a different module for each type of truck) of the second level network is selected. The same strain input data used in the first level is input into this module, divided into three networks that determine the output neurons corresponding to velocity, axle spacings and axle loads (Figure 3.10). The system is designed for a truck crossing the bridge on its own, but it could be extended to multiple

truck events by including a neural network at the front of the existing two levels. This additional network would uncouple the strain components of the different trucks.

Ideally, training patterns should be taken from strains measured as trucks pass over the bridge. A Fourier transform filter can remove dynamic effects from raw strain data, though the successful design of a filter in the time domain can reduce the overall time calculation. However, patterns based on experimental trials are inconvenient and time-consuming, and thus, only a few patterns can be obtained in this way. A theoretical bridge-truck model validated with real data collected from the bridge can provide a comprehensive set of training patterns that cover most regions of the problem domain. Though this theoretical bridge response involves errors, this approach is necessary if the system is to give accurate solution to any variation of the problem.

3.5.3 Extension to Orthotropic Bridges

Free of axle detector (FAD) algorithms have been developed for orthotropic bridges (OB-WIM) by Dempsey et al (1998a, 1999a). Velocity, number of axles and axle spacings are all calculated from the strain readings underneath the bridge at two different longitudinal locations. The values obtained for these parameters are not as accurate as axle detectors mounted on the road surface, but FAD systems are a solution to sites where installation of road sensors or road closure is not feasible. The prediction of axle and gross vehicle weights must allow for inaccurate estimates of axle spacings and velocity to some extent. This initial error is overcome using optimisation techniques.

Once a truck occurrence has been identified, the objective function to be minimised is the sum of squares of differences between the measured bending moments and the expected bending moments. The expected bending moment is generated from a theoretical model and it will depend on the truck parameters: Number of axles, velocity, axle spacing, axle weights and a parameter that aligns the measured response with the modelled response (offset).

This objective function must be examined with respect to certain truck parameters to determine an accurate optimisation procedure. The Hessian matrix was used to characterise the convexity of this function for a 2-axle rigid truck with axle spacings and weights as

parameters. It was found that while a simply supported beam is perfectly convex (only one minimum), there are multiple minima for a continuous beam (hence initial values in the optimisation procedure have a strong influence on final results). Figure 3.11(a) visualises the objective function of a 2-axle truck in a continuous beam where all parameters are maintained constant, except for the weight of the first axle and axle spacing. Figure 3.11(b) shows the objective function for a 5-axle truck on a continuous beam where the varying truck parameters are the axle spacings between the first three axles.

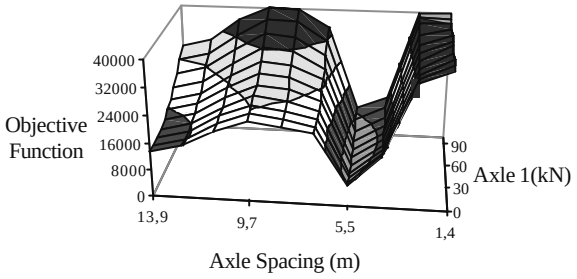

(a) Variation of Weight of First Axle and Axle Spacing (2-Axle Truck Objective Function)

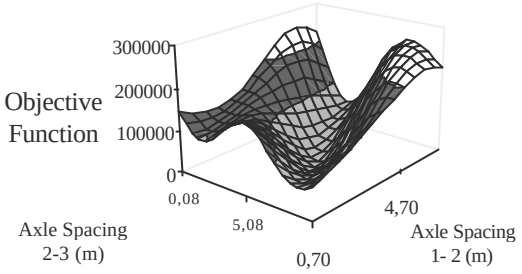

(b) Variation of Axle Spacing 1-2 and 2-3 (5-Axle Truck Objective Function)

Figure 3.11 – Evaluation of objective functions with respect to variation of truck parameters (after Dempsey et al. 1998a)

The correct minimum is more likely to be achieved if there is a good initial estimate of the truck parameters such as offset between measured and theoretical. It was found that the alignment of the first peak of the measured data with the first peak of the modelled data determines a sufficiently accurate value for the offset parameter. Errors in this parameter would generally result in small errors in axle weights and spacings. Hence, it was decided not to allow this parameter to vary in the optimisation to speed up calculations.

The optimisation problem was also extended to incorporate a 2-dimensional (2-D) bridge model, where each strain sensor at a different transverse location has a different influence line. In this case, the objective function to be minimised can be defined as (Dempsey et al. 2000):

$$O(p) = \sum_{j=1}^{S} \sum_{x=1}^{K} [M_j(x) - M_j{}^{M}(x)]^2 + k\left|p - p_0\right|^2 \tag{3.20}$$

where $M_j(x)$ and $M_j^M(x)$ are the theoretical and measured strains respectively at sensor j when the truck is at position x, S is the number of sensors transversely, K is the number of strain readings for a truck crossing, k a constant, and p_0 the initial values of the optimisation parameters p. The parameters p to be varied in the process are: velocity, axle spacings, axle weights and transverse location of the truck.

The OB-WIM algorithm first identifies a truck occurrence and calculates initial values of certain truck parameters. These first calculations are based on the distinct peaks left on the strain readings by the pass of each axle. If there is a correlation between the number of peaks and the time between different peaks at two instrumented sections, the number of axles are positively identified. If there is not a good correlation (i.e. problems in identifying closely spaced lightly loaded axles), a slightly modified algorithm is adopted that considers the possibility of a higher number of axles. A correct initial estimate of the velocity parameter is critical in finding the correct minimum. The time delay chosen for calculating speed is that which minimises the sum of squares of differences when superposing the measured responses at both sections. Initial values for axle spacings can be derived from this initial speed and the time between peaks in the measured record. Initial values for axle weights are taken as 30 kN (these parameters are not critical). Theoretical and measured responses are aligned prior to optimisation based on the first peak of the response, as stated earlier. Powell's method is recommended to carry out the optimisation constraining the speed parameter to a variation ± 5% with respect to the initial estimate. The solution is obtained when, for one iteration of the optimisation process, the change in the parameters is below a specified tolerance.

3.5.4 Multiple-longitudinal sensors

Kealy (1997) developed a weigh in motion system which is capable of giving a history of axle and gross vehicle weights at each point in time as a truck crosses a bridge at normal highway speed. This new bridge weigh in motion system is based on the use of multiple strain gauge sensor locations along the length of the bridge (MS-BWIM).

Principle

For the purpose of developing the required equations, the bridge will be assumed to act as a series of parallel longitudinal beams. This MS-BWIM system is based on a system of equations generated by assuming a static response of a bridge subjected to a vehicle loading. Bridge vibration is neglected in this instantaneous calculation (but truck vibration could be allowed for). The gross bending moment M at any longitudinal location along the span can be found by summing the individual bending moments as in Equation 3.3.

The bending moment at any point along the bridge for an N-axle vehicle can be expressed for any distance x of the first axle from the support, as a function of the influence line ($I(x)$) and applied loads (W_i) (Equation 3.4). In order to set up the necessary static equations, the bending moment influence line ($I_p(x)$) is required for each longitudinal sensor location p. For any truck crossing the bridge, a set of simultaneous equations as given in Equation 3.4 or 3.5 (as many as gauges) can be established for each point in position or time. Thus, a position or time based history of calculated axle weights can be determined.

The majority of trucks with four or more axles involve tandems, tridems or a combination of both. If we assume that all the axles within an axle group, whether a tandem or tridem, are of equal weight, we can reduce the number of unknowns when using Equation 3.5. This principle can be extended and applied to any vehicle where the number of individual axles exceeds the number of gauge locations. For most typical trucks, three gauge locations are adequate for the determination of axle weights. However, the equations must be independent and the number of axle groupings must be less than or equal to the number of independent equations.

Ideal Site

Single span bridges are not optimal for use with the MS-BWIM system as unique solutions to the generated simultaneous equations only occur for two axle vehicles when they are between the two strain gauge locations. As only two independent equations can be obtained, weights of a three-axle vehicle can not be obtained. Figure 3.12 shows influence lines and regions of dependence for three different strain gauges in a single span bridge (at ¼, ½ and ¾ span). All three gauges are dependent in Region I, while it is possible to find two independent gauges in Region II (between gauges 1 and 3).

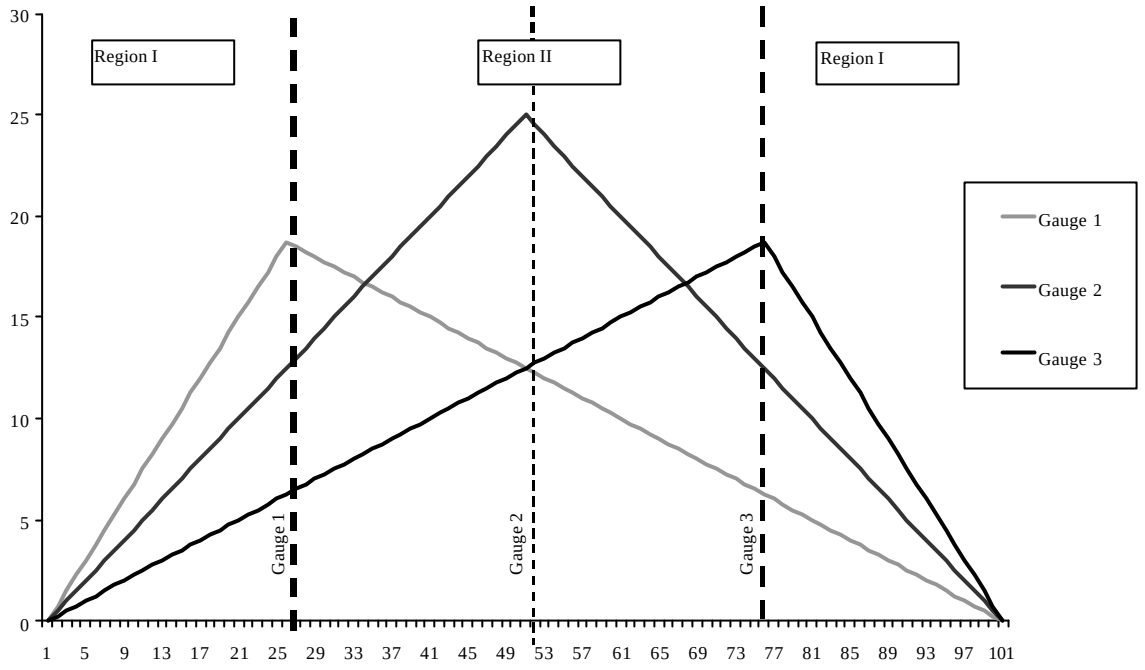

Figure 3.12 – Influence lines and regions of dependency in a single span

If a two span bridge is used, it is possible to determine weights for a 3-axle truck, but there are regions of the bridge where the determinant of the matrix of the equations equals or is approximately equal to zero, and axle weights can not be accurately calculated. Figure 3.13 shows influence lines and regions of dependency for strain at five gauge locations in a two-span bridge (at central support and ¼ and ¾ span from the central support). Only in region III (limited by gauges 2 and 4, located at ¼ span from the central support) there are three independent equations and instantaneous calculation of a three-axle truck becomes possible.

Kealy (1997) tested this algorithm on the two span continuous Belleville bridge on the A31 Motorway between Metz and Nancy in Eastern France. The calculated axle weights were very poor. This poor accuracy can, in part, be attributed to the manner in which velocity and the position of the vehicle on the bridge were monitored (a radar speed gun and a video camera) and the poor magnitudes of recorded strain.

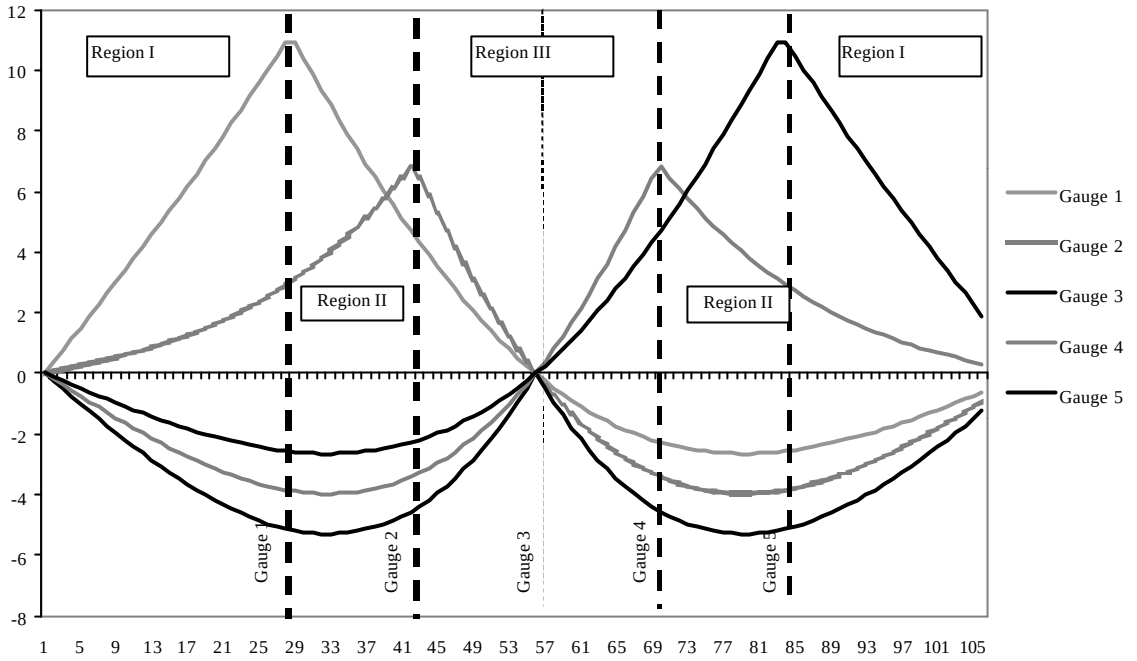

Figure 3.13 – Influence lines and regions of dependency in a two-span bridge

3.5.5 Combined System

Jacob et al (2000) introduces first theoretical studies on an algorithm that combines data from a pavement WIM system with continuous strain data taken from a B-WIM system. The algorithm minimises an error function given by the difference between theoretical and measured strain records in the B-WIM system (ε and $\tilde{\varepsilon}$ respectively), plus the difference between the real static axle weights and the calculated instantaneous axle weight by the WIM system (W_i and R_i respectively). This function is shown in Equation 3.21.

$$j = \frac{\lambda}{T}\sum_{k=1}^{T}\left[\varepsilon(t_k) - \tilde{\varepsilon}(t_k)\right]^2 + \frac{(1-\lambda)}{N}\sum_{i=1}^{N}\left[W_i - R_i(t_i)\right]^2 \qquad (3.21)$$

where T is the number of time increments for which strain is recorded on the bridge, N is the number of axles, and λ represents the relative weighting given to calculations of B-WIM compared to pavement WIM data. Thus, λ=0 represents a pure pavement WIM system, while λ=1 is a B-WIM system.

By minimising j with respect to W_i (setting all partial derivatives to zero), the axle weights can be predicted from the matrix formulation:

$$[H]\begin{bmatrix} W_1 \\ W_2 \\ \cdots \\ W_N \end{bmatrix} = \begin{bmatrix} \frac{\lambda}{T}\sum_{k=1}^{T}\tilde{\varepsilon}(t_k)I_1(t_k) + \frac{(1-\lambda)}{N}R_1(t_1) \\ \frac{\lambda}{T}\sum_{k=1}^{T}\tilde{\varepsilon}(t_k)I_2(t_k) + \frac{(1-\lambda)}{N}R_2(t_2) \\ \cdots \\ \frac{\lambda}{T}\sum_{k=1}^{T}\tilde{\varepsilon}(t_k)I_N(t_k) + \frac{(1-\lambda)}{N}R_N(t_N) \end{bmatrix} \tag{3.22}$$

where the square matrix *[H]* is given by:

$$[H] = \begin{bmatrix} \frac{\lambda}{T}\sum_{k=1}^{T}I_1(t_k)I_1(t_k) + \frac{(1-\lambda)}{N} & \frac{\lambda}{T}\sum_{k=1}^{T}I_2(t_k)I_1(t_k) & \cdots & \frac{\lambda}{T}\sum_{k=1}^{T}I_N(t_k)I_1(t_k) \\ \frac{\lambda}{T}\sum_{k=1}^{T}I_2(t_k)I_1(t_k) & \frac{\lambda}{T}\sum_{k=1}^{T}I_2(t_k)I_2(t_k) + \frac{(1-\lambda)}{N} & \cdots & \frac{\lambda}{T}\sum_{k=1}^{T}I_2(t_k)I_N(t_k) \\ \cdots & & & \\ \frac{\lambda}{T}\sum_{k=1}^{T}I_N(t_k)I_1(t_k) & \frac{\lambda}{T}\sum_{k=1}^{T}I_N(t_k)I_2(t_k) & \cdots & \frac{\lambda}{T}\sum_{k=1}^{T}I_N(t_k)I_N(t_k) + \frac{(1-\lambda)}{N} \end{bmatrix} \tag{3.23}$$

From theoretical studies based on the generation of randomly varying dynamic forces on a bridge, results showed that the bandwidth of the confidence interval of the error in axle weights decreases for a certain range of λ. Accuracy class in axle weights and Gross Vehicle Weights improved from B(10) for λ equal to 0 or 1 (this is, both WIM or B-WIM systems considered individually) to B(+7) for a combination corresponding to λ between 0.4 and 0.6.

3.6 DYNAMIC ALGORITHMS

Most operating algorithms are static, this is, based on linearity and static equations of equilibrium. As the data being recorded is the sum of static and dynamic components, the dynamic component is generally ignored. Bridge and truck dynamics have been proven to be one of the sources of inaccuracy of static algorithms. Traditional averaging or filtering techniques are not suitable for the removal of dynamics in every case. A need was identified by the author to include dynamics in some way inside the formulation of the algorithm. Some modern algorithms use equations of dynamic equilibrium that require as input the unfiltered measured data. Three different approaches are known: O'Connor & Chan (1988a, 1988b) develop a dynamic algorithm for the calculation of wheel loads based

on the use of multiple longitudinal locations. Ghosn & Xu present an algorithm to describe the varying dynamic axle load. Dempsey (1997, Dempsey et al. 1998b) calculates axle loads from a consideration of the first modal component of the applied force when measuring strains in one only longitudinal location. These three dynamic algorithms are described in the following sections.

3.6.1 O'Connor & Chan

O'Connor & Chan (1988a, 1988b) develop a dynamic B-WIM algorithm with the purpose of identifying high-impact vehicles on short span bridges. This algorithm is based on the measurement of strain at different longitudinal locations. Then, dynamic truck wheel loads are predicted from the bridge measurements. Two different types of bridge measurement are tested: displacements and strains. Through theoretical and laboratory tests, it is seen that the use of strains gives better estimates of dynamic load than displacements. The accuracy strongly depends on a good knowledge of the equivalent bending stiffness and strain-bending moment relationships.

First, the bridge is modelled as an assembly of n lumped masses interconnected by massless elastic beam elements. The measured displacement Y_i at node i can be expressed as in Equation 3.24.

$$Y_i = Y^A_i - Y^I_i - Y^D_i \tag{3.24}$$

where Y^A_i is the static displacement caused at node i by the applied loads, Y^I_i that due to the inertial forces and Y^D_i that due to the damping forces.

The displacement due to the applied load (Y^A_i) at node i is a function of the m applied wheel loads ($\{W\}_{mx1}$ = vector made of m rows and 1 column) that are on the bridge. This relationship is shown in Equation 3.25.

$$\{Y^A\}_{nx1} = [Y^u]_{nxm}\{W\}_{mx1} \tag{3.25}$$

where Y^u_{ij} represents the deflection at node i caused by a unit load acting at the position of the j^{th} load, not necessarily at node i.

The displacement Y^I_i due to the inertial forces can be expressed as equation 3.26.

$$\{Y^I\}_{nx1} = [Y^f]_{nxn}[m]_{nxn}\{\ddot{Y}\}_{nx1} \tag{3.26}$$

where $[Y^f]$ is the flexibility matrix relating nodal displacements and nodal loads, $[m]$ the mass matrix, and $\{\ddot{Y}\}$ the nodal accelerations.

In the assumption of Rayleigh viscous damping, the displacement Y^D_i can be formulated as:

$$\{Y^D\}_{nx1} = [Y^f]_{nxn}[C]_{nxn}\{\dot{Y}\}_{nx1} \tag{3.27}$$

where $[C]$ is the damping matrix and $\{\dot{Y}\}$ is the vector of velocity of nodal displacements.

The problem can also be expressed as a function of total bending moment M_i as given in Equation 3.28:

$$M_i = M^A_i - M^I_i - M^D_i \tag{3.28}$$

where:

$$\{M^A\} = [M^u]\{W\} \tag{3.29}$$

$$\{M^I\} = [M^f][m]\{\ddot{Y}\} \tag{3.30}$$

$$\{M^D\} = [M^f][C]\{\dot{Y}\} \tag{3.31}$$

The result is the equation that governs the dynamic problem. In terms of bending moment, this equation is given by:

$$\{M\} = [M^u]\{W\} - [M^f][m]\{\ddot{Y}\} - [M^f][C]\{\dot{Y}\} \tag{3.32}$$

Then, applied forces can be found from measured strain, displacements, velocities or accelerations. If displacements Y_i are to be measured, nodal velocities or accelerations can

be found by central numerical differentiation. This differentiation can lead to poor results due to discontinuities in Y_i as wheel loads traverse a node. In any event, there are significant practical difficulties in measuring deflections.

If accelerations $\ddot{Y}_i$ are to be measured, velocity or displacements can be found by integration. Results using nodal accelerations were badly affected by errors in the integration of accelerations (O'Connor & Chan 1988a). There is a possibility of occurrence of high frequency noise in the records, leading to errors in computed deflections and larger errors in the estimates of applied forces.

Velocity $\dot{Y}_i$ can be measured using velocimeters. The errors derived from obtaining displacements through integration of the velocity curve should not be as important as in the case of accelerations.

O'Connor & Chan state that predicted loads are much more sensitive to an error in the measurement of displacements than an error in the measurement of strains. Hence, strains are the preferred input data of O'Connor & Chan in the dynamic algorithm. However, the use of strains demands the establishment of a relationship between nodal displacements and nodal bending moments. This relationship that gives displacement as a function of strain, requires the unknown loads *W*. These loads are approximated by the values in the preceding time step. Then, velocities and accelerations are derived from these nodal displacements.

If accelerations, displacements or bending moment are known for all interior nodes at all times, then the number of knowns *n* will exceed the number of unknown applied forces, which generally requires a solution through a least-squares technique.

The choice of the sections to be instrumented has been proved to be important in final accuracy, i.e., avoiding undefined solutions due to zero nodal displacements or bending moments in some non-zero load cases. Based on common axle spacings of vehicles, O'Connor and Chan avoid zero nodal bending moment by an end element of less than 1 m, a second element less than 1.4 m, and an intermediate element less than 1.7 m. For a span length $L \geq 4.8$ m, the required number of elements *N* is given by:

$$N = INT\left(\frac{L-4.8}{1.7}\right)+5 \tag{3.33}$$

where L is span length.

Laboratory tests were carried out to confirm conclusions from theoretical analysis. This identified calibration as one of the most important factors in final accuracy. In particular:

- Determination of flexural stiffness of the beam (EI)
- Determination of calibration factors (C_F) relating bending moment and measured strains

The flexural stiffness (EI) and calibration factors (C_F) were obtained by comparing an increasing load at a fixed location to the measured displacement and the corresponding bending moment to the measured strain respectively. Static and dynamic calibrations based on the application of incremental load steps and sinusoidal loads at different frequencies respectively, were analysed. Agreement was found to be poor when the frequency of the sinusoidal load was close to the natural frequency of the beam. Best results in predictions were obtained when both calibration parameters were determined dynamically (O'Connor & Chan 1988b). This was due to the great sensitivity of EI to minor changes for this case.

3.6.2 Ghosn & Xu

Ghosn & Xu present a modified B-WIM algorithm that allows the calculation of the dynamic amplitude of the bridge vibration in addition to the axle weights of a truck as it crosses over a bridge. The unknown axle weights (W_i) are calculated by minimising an error function (j) given by the squared difference between a theoretical ($e(t)$) and a measured ($\tilde{e}(t)$) strain record as in Equation 3.34.

$$j = \left[e(t) - \tilde{e}(t)\right]^2 \tag{3.34}$$

The algorithm starts by finding dominant frequencies (f_i) using a Fourier analysis of the strain record of an end girder. These end girders usually carry little static but considerable

dynamic effect. This makes it easier to distinguish between the static components and the purely dynamic components of the Fourier Transform.

The theoretical strain record ($e(t)$) is made up of two components: A static component related to the influence line ($I(t)$) and a dynamic component given by "dynamic influence lines" of different frequencies f_i. Equation 3.35 shows this approach:

$$e(t) = \sum_{i=1}^{N} W_i I_i(t) + \sum_{i=1}^{N_f} (D^s{}_i \sin(w_i t) + D^c{}_i \cos(w_i t)) \tag{3.35}$$

where N is number of axles, N_f is number of frequencies, $w_i = 2pf_i$ is circular frequency, and $D^s{}_i$ and $D^c{}_i$ are the amplitudes of the sine and cosine waves for the i^{th} frequency, respectively. These amplitudes and the axle weights are unknown and they are calculated by minimising j (Equation 3.34) with respect to W_i, $D^s{}_i$ and $D^c{}_i$ as shown in Equations 3.36 to 3.39.

$$\frac{\partial j}{\partial W_i} = 0 \qquad i = 1,\ldots,N \tag{3.36}$$

$$\frac{\partial j}{\partial D^s{}_i} = 0 \qquad i = 1,\ldots,N_f \tag{3.37}$$

$$\frac{\partial j}{\partial D^c{}_i} = 0 \qquad i = 1,\ldots,N_f \tag{3.38}$$

This results in a matrix formulation given by:

$$\begin{bmatrix}
I_1I_1 & I_1I_2 & \ldots & I_1\sin(w_1t_j) & I_1\sin(w_2t_j) & \ldots & I_1\cos(w_1t_j) & I_1\cos(w_2t_j) & \ldots \\
I_2I_1 & I_2I_2 & \ldots & I_2\sin(w_1t_j) & I_2\sin(w_2t_j) & \ldots & I_2\cos(w_1t_j) & I_2\cos(w_2t_j) & \ldots \\
\ldots & & & & & & & & \\
\sin(w_1t_j)I_1 & \sin(w_1t_j)I_2 & \ldots & \sin(w_1t_j)\sin(w_1t_j) & \sin(w_1t_j)\sin(w_2t_j) & \ldots & \sin(w_1t_j)\cos(w_1t_j) & \sin(w_1t_j)\cos(w_2t_j) & \ldots \\
\sin(w_2t_j)I_1 & \sin(w_2t_j)I_2 & \ldots & \sin(w_2t_j)\sin(w_1t_j) & \sin(v_2t_j)\sin(w_2t_j) & \ldots & \sin(w_2t_j)\cos(w_1t_j) & \sin(w_2t_j)\cos(w_1t_j) & \ldots \\
\ldots & & & & & & & & \\
\cos(w_1t_j)I_1 & \cos(w_1t_j)I_2 & \ldots & \cos(w_1t_j)\sin(w_1t_j) & \cos(w_1t_j)\sin(w_2t_j) & & \cos(w_1t_j)\cos(w_1t_j) & \cos(w_1t_j)\cos(w_2t_j) & \ldots \\
\cos(w_2t_j)I_1 & \cos(w_2t_j)I_2 & \ldots & \cos(w_2t_j)\sin(w_1t_j) & \cos(v_2t_j)\sin(w_2t_j) & & \cos(w_2t_j)\cos(w_1t_j) & \cos(v_2t_j)\cos(w_2t_j) & \ldots \\
\ldots & & & & & & & &
\end{bmatrix}
\begin{Bmatrix} W_1 \\ W_2 \\ \ldots \\ D^s{}_1 \\ D^s{}_2 \\ \ldots \\ D^c{}_1 \\ D^c{}_2 \\ \ldots \end{Bmatrix}
=
\begin{Bmatrix} \tilde{e}I_1 \\ \tilde{e}I_2 \\ \ldots \\ \tilde{e}\sin(w_1t_j) \\ \tilde{e}\sin(w_2t_j) \\ \ldots \\ \tilde{e}\cos(w_1t_j) \\ \tilde{e}\cos(w_2t_j) \\ \ldots \end{Bmatrix} \tag{3.39}$$

Initial results show that this method is capable of estimating the dynamic response of highway bridges under random truck crossings by extending the B-WIM algorithm as

proposed by Moses. However, the method is limited when a significant dynamic component and the static component of the Fourier Transform have similar frequencies. In this case, some of the static component might be included in the estimate of the dynamic amplitude or vice versa and the algorithm will be inaccurate.

3.6.3 Dempsey

Dempsey (1997, 1998b) introduced a new dynamic algorithm based on a single longitudinal sensor location. His algorithm determines axle weights by minimising an error function given by the squared difference between experimental and theoretical approximations of the first modal component of the applied force ($\tilde{F}_1$ and F_1 respectively) as follows:

$$j = \sum_{k=1}^{T} [F_1(t_k) - \tilde{F}_1(t_k)]^2 \tag{3.40}$$

The first modal component of the applied force $\tilde{F}_1$ can be estimated from measurements that are normalised (divided by bridge modal mass m_1) as given in Equation 3.41:

$$\frac{\tilde{F}_1(t_k)}{m_1} = \ddot{y}_1(t_k) + 2\zeta_1\omega_1\dot{y}_1(t_k) + \omega_1^2 y_1(t_k) \tag{3.41}$$

where ω_1 is the modal circular frequency and ζ_1 the modal damping ratio. This equation, derived from the fundamental equation of dynamics and modal decoupling, requires generalised displacements y_1. Velocities ($\dot{y}_1$) and accelerations ($\ddot{y}_1$) can be obtained by differentiation. However, strains are generally measured instead of displacements. In this case, displacements can be approximated by integrating the bending moment diagram suggested by the measured strain. This calculation requires an iterative process until the difference between the results in applied loads from two successive calculations is small enough.

The theoretical modal component of the applied force is obtained through multiplication of the applied load by the value of the bridge mode shape at that load location (Equation 3.42).

$$F_1(t_k) = \{\Phi\}^T \{F(t_k)\} \tag{3.42}$$

where $\{\boldsymbol{F}_i\}$ is a vector containing the values of the mode shape ordinate at the strain gauge location for the position of axle i at instant t_k.

By minimising error function defined in Equation 3.40:

$$\frac{\partial \boldsymbol{j}}{\partial F_{1j}} = 0 \qquad ; \qquad j = 1,2,\ldots N \tag{3.43}$$

where N is number of axles.

This gives:

$$\sum_{k=1}^{T}[2(\sum_{i=1}^{N} F_{1_i}\Phi_1(t_k - \frac{\sum_{r=1}^{i-1} a_r}{v}) - \tilde{F}_1(t_k))\Phi_1(t_k - \frac{\sum_{r=1}^{j-1} a_r}{v})] = 0 \quad ; \quad j = 1,2,\ldots,N \tag{3.44}$$

where v is velocity and a_j is axle spacing between axle j and $j+1$ (Figure 3.2).

And re-ordering:

$$\sum_{k=1}^{T}\left[\sum_{i=1}^{N} F_{1i}\Phi_1(t_k - \frac{\sum_{r=1}^{i-1} a_r}{v})\right]\Phi_1(t_k - \frac{\sum_{r=1}^{j-1} a_r}{v}) = \sum_{k=1}^{T}\tilde{F}_1(t_k)\Phi_1(t_k - \frac{\sum_{r=1}^{j-1} a_r}{v}) \quad ; \quad j = 1,\ldots,N \tag{3.45}$$

This least squares fitting method between F_1 and $\tilde{F}_1$ let derive a matrix formulation as:

$$[H]_{NxN} * \{F_1\}_{Nx1} = \{P\}_{Nx1} \tag{3.46}$$

where $\{F_1\}$ are the first modal component of the applied force and n number of axles. $\{F_1\}$ is assumed to be related to the axle weights through a calibration factor. The matrix $[H]$ and vector $\{P\}$ are defined as :

$$\left[H_{ij}\right] = \sum_{k=1}^{t} \Phi_1(t_k - \frac{\sum_{r=1}^{i-1} a_r}{v}) \Phi_1(t_k - \frac{\sum_{r=1}^{j-1} a_r}{v}) \tag{3.47}$$

$$\left\{P_j\right\} = \sum_{k=1}^{t} \frac{\tilde{F}_1(t_k) \Phi_1(t_k - \frac{\sum_{r=1}^{j-1} a_r}{v})}{m_1} \quad ; \quad j = 1,..,N \tag{3.48}$$

Dempsey et al (1998b) reveal the potential of a dynamic B-WIM algorithm for bridges with short spans and high dynamics in the measured record. However, the author addresses some shortcomings in this algorithm:

- The first modal component of the force is estimated by applying the decoupled equation of dynamics for the first bridge mode shape (Equation 3.41). This equation requires displacements, velocity and accelerations. Additionally, bridge modal mass, modal damping and frequency for that mode shape are necessary. As strains are generally measured instead of deflections, some errors will result from integration of the bending moment diagram.
- As the algorithm is based on one longitudinal sensor location, the shape of the bending moment diagram is assumed and the diagram reconstructed from the strain measurements at one single longitudinal location. Additionally, the bending effect of damping and inertial forces is ignored in the bending moment diagram. Though convergence might arise after a few iterations, the final result could be quite far from the static value due to the inaccuracy of the bending moment diagram.
- Another error is introduced by the use of total displacements in a modal equation (Equation 3.41) that requires generalised displacements corresponding to a specific mode shape.
- The algorithm assumes that the first modal component of the applied forces and the static weights are directly related, which can clearly differ from reality. If a series of

concentrated loads are represented by the modal components of the bridge vibration (this is, the sum of the products of the load magnitude and the value of the mode shape at the load location for each load), the most significant contribution is not going to be made by the first modal component at every instant. The highest modal component will depend on the axle spacing, applied load, bridge length and vehicle location. In other words, only one modal component (not always the most representative) is used to represent a force, and hence, an incorrect assumption of proportionality between this single representation and the force is made.

3.7 ACCURACY OF BRIDGE WEIGH IN MOTION SYSTEMS

Traditionally, B-WIM systems were recommended for culverts or bridges with spans between 8 and 25 m. Work was necessary to establish which bridge types could effectively serve for weigh-in-motion purposes. The COST323 action and the WAVE project have tested B-WIM systems in cold climates and for a wide range of bridges, i.e. short slab bridges, integral bridges and orthotropic deck bridges. Results of different test trials prior to WAVE and as part of WAVE (Jacob et al. 2000) are presented in this section. It has also been proven that different types of bridge can be used without axle detectors mounted on the road surface (Ž nidaric et al. 1999a).

3.7.1 American, Australian and European Bridge WIM prior to WAVE

In Australia, CULWAY has been found to typically estimate static gross vehicle weight within ±10%, and the individual axle weights within ±15% at 95% confidence limits[10]. Tierney et al (1996) found similar accuracy of two pavement WIM (Australian plate in ground on load cells and German strain gauged plate in ground) and three B-WIM systems (CULWAY, AXWAY and FASTWEIGH), with poorer results from a pavement WIM based on a surface mounted capacitive weigh pad, which is not flushed with the road surface.

All accuracy classification until the end of the chapter is given according to the COST323 Specification (1997). In 1995, a European (first DuWIM) and a commercially available American B-WIM system were first tested together on a bridge in Slovenia (O'Brien et al. 1999b). Both systems were giving an accuracy class of D+(20) for gross vehicle weights,

but when considering single axle and axle group results, only an accuracy class E was achieved.

3.7.2 Slovenia

B-WIM tests have been carried out in Slovenia as part of the WAVE project. The study centred on concrete slab bridges. Final accuracy was found to be strongly related to a number of parameters (Section 3.5.1) such as: influence line, calibration methods, velocity, road unevenness and bridge skew. Žnidaric et al (1999b) report on the influence of these parameters on final accuracy, which results are summarised in this section. The B-WIM system being used for analysis is referred to as SiWIM (Žnidaric et al. 1998), which is briefly described in Chapter 4. The SiWIM software uses Moses' algorithm as the basis for the calculation of axle weights.

Influence of Influence line

A 10 m span, 9° skew integral slab bridge was investigated. A common calibration factor was obtained from a test vehicle and applied to all vehicles. If the theoretical influence line for a single fixed (encastré) supported span is taken, the accuracy class retained is D(25) due mainly to inaccuracy in single axles. B(10) and C(15) accuracy are obtained respectively for the individual criteria of group of axles and gross weight. These results can be improved by using an experimental influence line based on the measured strains, which has become common practice (McNulty 1999). Thanks to a better accuracy in single axles, the overall accuracy is raised to D+(20). The results are presented in Table 3.1.

Table 3.1 – Accuracy classification for experimental influence line

(**n**: Total number of vehicles; **m**: mean; **s**: Standard deviation; $\mathbf{p_0}$: level of confidence; **d**: tolerance of the retained accuracy class; $\mathbf{d_{min}}$: minimum width of the confidence interval for π_0; **p**: Level of confidence of the interval $[-\delta,\delta]$)

	Relative error statistics				Accuracy calculation				
Criterion	**n**	**m (%)**	**s (%)**	**p_0 (%)**	**Class**	**d (%)**	**d_{min} (%)**	**p (%)**	**Class Retained**
Single axle	60	2.71	9.81	91.8	D+(20)	25	20.52	91.6	**D+(20)**
Group of axles	18	-1.05	4.26	86.5	B+(7)	10	8.99	89.1	
Gross Weight	31	1.59	5.48	89.8	C(15)	15	11.62	89.3	

Influence of Calibration Methods

Accuracy can be improved by using different calibration factors for different vehicle types. If two calibrations factors are adopted, the overall accuracy improves from the previous D+(20) to C(15).

Influence of Velocity

The effect of a bad first estimation of speed can be overcome with the use of optimisation techniques (Sections 3.5.1 and 3.5.3). The accuracy classification when applying two calibration factors, experimental influence lines and optimisation, is given in Table 3.2. Compared to the last results, optimisation brings gross weight from C(15) up to B(10). This improvement will be more important if estimation of speed is not good in first instance.

Table 3.2 – Accuracy classification with 2 calibration factors and optimisation

(**n**: Total number of vehicles; **m**: mean; **s**: Standard deviation; $\mathbf{p_0}$: level of confidence; **d**: tolerance of the retained accuracy class; $\mathbf{d_{min}}$: minimum width of the confidence interval for π_0; **p**: Level of confidence of the interval $[-\delta,\delta]$)

	Relative error statistics				Accuracy calculation				
Criterion	**n**	**m (%)**	**s (%)**	**p_o (%)**	**Class**	**d (%)**	**d_{min} (%)**	**p (%)**	**Class Retained**
Single axle	60	1.41	7.59	91.8	C(15)	20	15.61	97.73	**C(15)**
Group of axles	18	-2.40	4.16	86.5	B+(7)	10	9.53	88.75	
Gross Weight	31	-0.09	4.63	89.8	B(10)	10	9.50	91.72	

Finally, overall accuracy can be brought up to B(10) with a 4% fixed redistribution of load from the first axle to the others in vehicles with more than 2 axles. This approach is similar to the calibration by axle rank discussed in Section 2.4.4.

Influence of Road Evenness

A similar bridge to the one above, but with a bump on the bridge, has been tested experimentally by Žnidaric et al (1999b). This bump induced considerable excitation of truck wheel loads and, even though accuracy in gross weight remains as B(10), the overall accuracy is E(40) as shown in Table 3.3. However, if all axles below 20 kN are ignored, the overall accuracy is improved to C(15). These axles and group of axles show a high bias

in results for single axles and group of axles. This indicates that better results could be obtained if using an additional calibration by axle rank.

Table 3.3 – Accuracy classification for bridge with bump

(**n**: Total number of vehicles; **m**: mean; **s**: Standard deviation; $\mathbf{p_0}$: level of confidence; **d**: tolerance of the retained accuracy class; $\mathbf{d_{min}}$: minimum width of the confidence interval for π_0; **p**: Level of confidence of the interval $[-\delta,\delta]$)

	Relative error statistics				Accuracy calculation				
Criterion	**No**	**Mean (%)**	**St.D. (%)**	$\mathbf{p_0}$ **(%)**	**Class**	**d (%)**	$\mathbf{d_{min}}$ **(%)**	**p (%)**	**Class Retained**
Single axle	52	-6.22	7.86	96.2	D(25)	30	28.4	97.32	**E(40)**
Group of axles	32	6.94	11.85	95.4	E(40)	43	40.28	96.84	
Gross Weight	34	0.00	3.23	95.5	B(10)	10	9.82	95.92	

Influence of Bridge Skewness

Two integral slab bridges, each with two spans of about 10 m, were used to check how skew could affect accuracy. They are very similar except for their skewness, which was 7° and 26°. Results are presented in Table 3.4.

Table 3.4 – Effect of bridge skew on accuracy classification

(**n**: Total number of vehicles; **m**: mean; **s**: Standard deviation; $\mathbf{p_0}$: level of confidence; **d**: tolerance of the retained accuracy class; $\mathbf{d_{min}}$: minimum width of the confidence interval for π_0; **p**: Level of confidence of the interval $[-\delta,\delta]$)

	Relative error statistics				Accuracy calculation				
7° Skew / **Criterion**	**n**	**m (%)**	**s (%)**	$\mathbf{p_0}$ **(%)**	**Class**	**d (%)**	$\mathbf{d_{min}}$ **(%)**	**p (%)**	**Class retained**
Single axle	31	5.24	8.32	89.8	C(15)	20	19.46	90.89	**C(15)**
Group of axles	33	-0.84	4.77	90.0	B+(7)	10	9.89	90.43	
Gross Weight	32	0.43	3.17	89.9	B+(7)	7	6.55	92.31	
	Relative error statistics				**Accuracy calculation**				
26° Skew / **Criterion**	**n**	**m (%)**	**s (%)**	$\mathbf{p_0}$ **(%)**	**Class**	**d (%)**	$\mathbf{d_{min}}$ **(%)**	**p (%)**	**Class retained**
Single axle	27	7.29	9.26	89.3	D+(20)	25	22.96	92.69	**D+(20)**
Group of axles	37	2.20	4.24	90.3	B+(7)	10	9.5	92.17	
Gross Weight	32	2.84	3.53	89.9	B(10)	10	8.78	94.62	

The inaccuracy for the criterion of single axles is related to the fact that most of them corresponded to very lightly loaded steering axles. Once again, this could be improved if using calibration by axle rank due to the significant bias in single axles. In conclusion, slab bridges were found suitable for B-WIM measurements with accuracy comparable to beam bridges (Žnidaric et al 1999b).

3.7.3 Autreville

Tests on orthotropic steel bridges took place in Autreville, Eastern France, as part of the WAVE project (Section 2.2), during August 1997 and July 1998. Two longitudinal sections were instrumented with strain sensors at seven different transverse locations (on each of the seven stiffeners under the slow lane). Dempsey et al (1999a) carried out the analysis by implementing the OB-WIM algorithm described in Section 3.5.3. When using an optimisation algorithm based on a 1-dimensional bridge model, accuracy class D+(20) was achieved for all criteria. This accuracy was raised to C(15) when considering both longitudinal and transverse directions were represented (2-D model). This accuracy class was achieved without any axle detectors on the road surface. The results for this second approach are shown in Table 3.5.

Table 3.5 – Accuracy classification for orthotropic bridge

(**n**: Total number of vehicles; **m**: mean; **s**: Standard deviation; $\mathbf{p_0}$: level of confidence; **d**: tolerance of the retained accuracy class; $\mathbf{d_{min}}$: minimum width of the confidence interval for π_0; **p**: Level of confidence of the interval $[-\delta,\delta]$)

	Relative error statistics				Accuracy calculation				
Criterion	**n**	**m (%)**	**s (%)**	**p_0 (%)**	**Class**	**d (%)**	**d_{min} (%)**	**p (%)**	**Class Retained**
Single axle	55	0.79	8.95	91.6	C(15)	20	18.3	91.6	**C(15)**
Group of axles	27	0.17	8.22	89.1	C(15)	18	16.9	89.1	
Gross Weight	28	0.55	5.55	89.3	C(15)	15	11.5	89.3	

3.7.4 Luleå Tests in Cold Environment

B-WIM measurements performed by TCD (Trinity College Dublin) took place in June 1997, March and June 1998 as part of the Cold Environmental Test in Luleå (Section 2.5.5). The B-WIM system was re-installed and re-calibrated each time. Data was filtered at 4 Hz in the first two tests, while data remained unfiltered in the third test. The bridge is

an integral structure composed of two spans, 14.6 m each. UCD (**U**niversity **C**ollege **D**ublin) and ZAG (Slovenian National Building and Civil Engineering Institute) carried out analysis of the measured data independently. Though both Dublin (DuWIM) and Slovenian (SiWIM) approaches use a static algorithm similar to the one proposed by Moses, one of their differences lies in the adjustment of the influence line taken as the reference.

Different bridge behaviour (influence line) was detected in the Summer and Winter seasons, perhaps due to the extreme weather conditions (river frozen around the columns of the bridge). Final accuracy has been achieved by detecting and removing those vehicles with anomalies (i.e. wrong identification of the vehicle being weighed in the static scale and recordings interfered with, either electronically or by a multiple vehicle presence). From analysis of the Winter results, the daily temperature fluctuation was found to have a significant effect as shown in Figure 3.14. This was due to a difference in temperature between the active gauge (on the bridge) and the dummy gauge (in the data acquisition equipment in a car). When allowing for a temperature correction, results for random traffic improved from an overall accuracy of D+(20) to C(15). Best results were achieved in June 1998 due to the use of unfiltered data, a new gauge configuration all located on the bridge and a better data acquisition card (16 bits instead of 12 bits) which improved strain amplification by nearly 10.

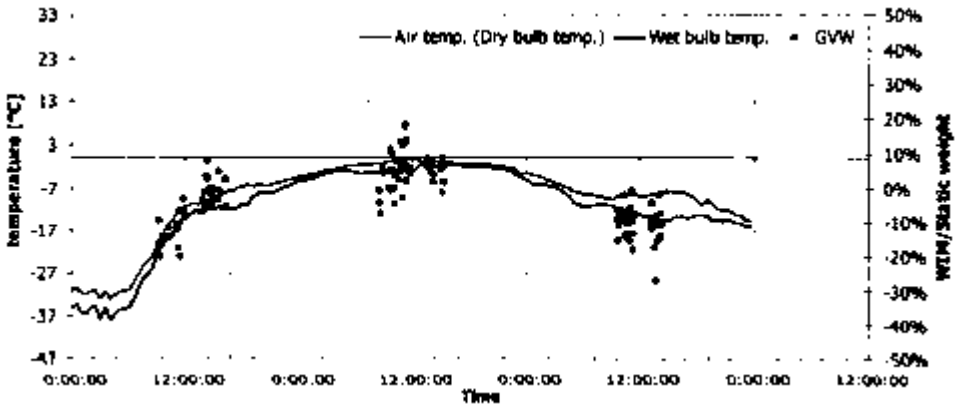

Figure 3.14 – Temperature dependence of Luleå B-WIM measurements (after Žnidaric et al 1999b)

ZAG

Results from test vehicles and random traffic for the first two tests were found by ZAG to be C(15). The results corresponding to the calibration of the second summer season are shown in Table 3.6.

Table 3.6 – Accuracy classification for test vehicles in June 1998

(**n**: Total number of vehicles; **m**: mean; **s**: Standard deviation; $\mathbf{p_0}$: level of confidence; **d**: tolerance of the retained accuracy class; $\mathbf{d_{min}}$: minimum width of the confidence interval for π_0; **p**: Level of confidence of the interval $[-\delta,\delta]$)

	Relative error statistics				Accuracy calculation				
Criterion	**n**	**m (%)**	**s (%)**	**p_0 (%)**	**Class**	**d (%)**	**d_{min} (%)**	**p (%)**	**Class Retained**
Single axle	34	0.32	4.27	95.5	B(10)	15	13.00	98.05	**B(10)**
Group of axles	54	0.01	2.57	96.2	B+(7)	10	7.72	99.36	
Gross Weight	34	0.00	2.30	95.5	B+(7)	7	7.00	95.50	

When the population from random traffic was analysed first, results were class D(25), surprisingly. Further analysis showed that there was a mismatch between the vehicles weighed by the B-WIM system and the static scale. Removing the outliers, B+(7) was obtained over a total sample of 104 vehicles. However, the system remained in B(10) because of the criterion of group of axles and single axles (Table 3.7).

Table 3.7 – Accuracy classification for random traffic in June 1998

(**n**: Total number of vehicles; **m**: mean; **s**: Standard deviation; $\mathbf{p_0}$: level of confidence; **d**: tolerance of the retained accuracy class; $\mathbf{d_{min}}$: minimum width of the confidence interval for π_0; **p**: Level of confidence of the interval $[-\delta,\delta]$)

	Relative error statistics				Accuracy calculation				
Criterion	**n**	**m (%)**	**s (%)**	**p_0 (%)**	**Class**	**d (%)**	**d_{min} (%)**	**p (%)**	**Class Retained**
Single axle	187	0.75	6.42	93.7	B(10)	15	13.00	96.9	**B(10)**
Group of axles	191	-0.86	5.75	93.7	B(10)	13	11.7	96.2	
Gross Weight	104	-0.03	2.83	92.9	B+(7)	7	5.7	97.5	

UCD

McNulty (1999) obtains accuracy classes of C(15), C(15) and B(10) for the three respective tests. The reduced accuracy in the first two trials is due to the effects of low pass filtering (already discussed in Section 3.5.1). Detailed results of the three tests for random traffic are shown in Tables 3.8 to 3.10.

Table 3.8 – Accuracy classification for random traffic in June 1997

(**n**: Total number of vehicles; **m**: mean; **s**: Standard deviation; $\mathbf{p_0}$: level of confidence; **d**: tolerance of the upper accuracy class; $\mathbf{d_n}$: tolerance of the lower accuracy class; **p**: Level of confidence of the interval of the retained accuracy class)

	Relative error statistics				Accuracy calculation				
Criterion	**n**	**m (%)**	**s (%)**	$\mathbf{p_o}$ **(%)**	**Class**	**d** B(10)	$\mathbf{d_n}$ C(15)	**p (%)**	**Class Retained**
Single axle	156	1.318	8.562	93.5	C(15)	15	20	96.8	**C(15)**
Group of axles	162	3.7	6.02	93.6	C(15)	13	18	98.6	
Gross Weight	95	3.09	4.08	92.8	B(10)	10	10	93.1	

Table 3.9 – Accuracy classification for random traffic in March 1998

(**n**: Total number of vehicles; **m**: mean; **s**: Standard deviation; $\mathbf{p_0}$: level of confidence; **d**: tolerance of the upper accuracy class; $\mathbf{d_n}$: tolerance of the lower accuracy class; **p**: Level of confidence of the interval of the retained accuracy class)

	Relative error statistics				Accuracy calculation				
Criterion	**n**	**m (%)**	**s (%)**	$\mathbf{p_o}$ **(%)**	**Class**	**d** C(15)	$\mathbf{d_n}$ D(20)	**p (%)**	**Class Retained**
Single axle	188	-0.757	8.562	94.5	C(15)	20	25	97.09	**C(15)**
Group of axles	227	-1.904	8.325	94.9	C(15)	18	23	95.23	
Gross Weight	125	-1.008	6.373	94.4	C(15)	15	20	96.84	

Table 3.10 – Accuracy classification for random traffic in June 1998

(**n**: Total number of vehicles; **m**: mean; **s**: Standard deviation; $\mathbf{p_0}$: level of confidence; **d**: tolerance of the upper accuracy class; $\mathbf{d_n}$: tolerance of the lower accuracy class; **p**: Level of confidence of the interval of the retained accuracy class)

	Relative error statistics				Accuracy calculation				
Criterion	**n**	**m (%)**	**s (%)**	**p_o (%)**	**Class**	**d B(7)**	**d_n B(10)**	**p (%)**	**Class Retained**
Single axle	188	-1.312	7.267	93.7	B(10)	11	25	94.12	**B(10)**
Group of axles	239	-0.885	3.72	95.4	B(10)	10	13	98.08	
Gross Weight	122	-0.182	5.259	93.2	B(10)	7	10	98.54	

3.8 CONCLUSIONS

B-WIM was developed by Moses (Section 3.3) in the 1970's as an alternative to pavement WIM systems. These systems convert the information provided by bridge measurements into traffic data through the application of an algorithm. First algorithms were based on static equations of equilibrium and the concept of influence line. These systems were recommended in beam & slab bridges initially, and they were successfully implemented in culverts in the 1980's (Section 3.4.2). However, the use of B-WIM in other bridge forms was not always feasible due to durability problems of axle detectors embedded in or mounted on the road surface, bridge and truck dynamics and errors derived from the estimation of axle spacing, speed and/or influence line (Section 3.5.1).

In recent years, the use of optimisation techniques (Section 3.5.3) and experimental influence lines have overcome some of these limitations. So, B-WIM has been extended to slab (Section 3.7.2) and orthotropic bridges (Section 3.7.3), and a B-WIM system installed in a two-span integral bridge has achieved excellent levels of accuracy in a major trial test under extreme climate conditions (Section 3.7.4). The use of more sensors (Section 3.5.4), neural networks (Section 3.5.2) and dynamic equations of equilibrium (Section 3.6) are expected to further improve the accuracy, durability and range of applicability of B-WIM.